

1 The suspended small-particles layer in the oxygen-poor Black Sea: a 2 proxy for delineating the effective N₂-yielding section

3 Rafael Rasse¹, Hervé Claustre¹, and Antoine Poteau¹

4 ¹Sorbonne Université and CNRS, Laboratoire d'Océanographie de Villefranche (LOV) UMR7093, Institut de la Mer de
5 Villefranche (IMEV), 06230, Villefranche-sur-Mer, France.

6
7 Correspondence to: rafael.rasse@obs-vlfr.fr; rjrasse@gmail.com

8 **Abstract.** The shallower oxygen-poor water masses of the ocean confine a majority of the microbial communities that can
9 produce up to 90% of oceanic N₂. This effective N₂-yielding section encloses a suspended small-particle layer, inferred from
10 particle backscattering (b_{bp}) measurements. It is thus hypothesized that this layer (hereafter, the b_{bp} -layer) is linked to microbial
11 communities involved in N₂-yielding such as nitrate-reducing SAR11 as well as sulphur-oxidizing, anammox and denitrifying
12 bacteria — a hypothesis yet to be evaluated. Here, data collected by three BGC-Argo floats deployed in the Black Sea are used
13 to investigate the origin of this b_{bp} -layer. To this end, we evaluate how the key drivers of N₂-yielding bacteria dynamics impact
14 on the vertical distribution of b_{bp} and the thickness of the b_{bp} -layer. In conjunction with published data on N₂ excess, our results
15 suggest that the b_{bp} -layer is at least partially composed of the bacteria driving N₂ yielding for three main reasons: (1) strong
16 correlations are recorded between b_{bp} and nitrate; (2) the top location of the b_{bp} -layer is driven by the ventilation of oxygen-
17 rich subsurface waters, while its thickness is modulated by the amount of nitrate available to produce N₂; (3) the maxima of
18 both b_{bp} and N₂ excess coincide at the same isopycnals where bacteria involved in N₂ yielding coexist. We thus advance that
19 b_{bp} and O₂ can be exploited as a combined proxy to delineate the N₂-yielding section of the Black Sea. This proxy can
20 potentially contribute to refining delineation of the effective N₂-yielding section of oxygen-deficient zones via data from the
21 growing BGC-Argo float network.

22 1 Introduction

23 Oxygen-poor water masses (O₂ < 3 μM) host the microbial communities that produce between 20-40% of oceanic N₂ mainly
24 via heterotrophic denitrification and anaerobic oxidation of ammonium (Gruber and Sarmiento, 1997; Devries et al. 2013;
25 Ward 2013). The shallower oxygen-poor water masses (~50-200 m) are the most effective N₂-producing section because this
26 is where the microbial communities that condition the process mainly develop and generate up to 90% of the N₂ (Ward et al.,
27 2009; Dalsgaard et al., 2012; Babin et al., 2014). These microbial communities include nitrate-reducing SAR11, and anammox,
28 denitrifying, and sulphur-oxidizing bacteria (e.g. Canfield et al., 2010; Ulloa et al., 2012; Ward 2013; Tsementzi et al., 2016;
29 Callbeck et al., 2018). It is thus important to unravel the biogeochemical parameters that trigger the accumulation of such
30 bacteria in the ocean's oxygen-poor water masses. This information is crucial for understanding and quantifying how bacterial
31 biomass and related N₂ yielding bacteria can respond to the ongoing expansion of oceanic regions with low oxygen (Keeling
32 and Garcia, 2002; Stramma et al., 2008; Helm et al., 2011; Schmidtko et al., 2017). Ultimately, greater accuracy in this domain
33 can contribute to improving mechanistic predictions on how such expansion affects the oceans' role in driving the Earth's
34 climate by sequestering atmospheric carbon dioxide (e.g. Oschlies et al., 2018).

35 In oxygen-poor water masses, the biogeochemical factors that can affect the abundance of denitrifying and anammox bacteria
36 are the levels of O₂, organic matter (OM), nitrate (NO₃⁻), ammonium (NH₄⁺), and hydrogen sulfide (H₂S) (Murray et al., 1995;

37 Ward et al., 2008; Dalsgaard et al., 2014; Bristow et al., 2016). Therefore, to elucidate what triggers the confinement of such
38 bacteria, we need to investigate how the above biogeochemical factors drive their vertical distribution, with high temporal and
39 vertical resolution. To this end, we should develop multidisciplinary approaches that allow us to permanently monitor the full
40 range of biogeochemical variables of interest in oxygen-poor water masses.

41 Optical proxies of tiny particles can be applied as an alternative approach to assess the vertical distribution of N₂-yielding
42 microbial communities in oxygen-poor water masses (Naqvi et al., 1993). For instance, nitrate-reducing SAR11, and
43 anammox, denitrifying, and sulphur-oxidizing bacteria are found as free-living bacteria (0.2-2 µm), and can be associated with
44 small suspended (> 2-30 µm), and large sinking (> 30 µm) particles (Fuchsman et al., 2011, 2012a, 2017; Ganesh et al., 2014,
45 2015). Therefore, particle backscattering (b_{bp}), a proxy for particles in the ~0.2-20 µm size range (Stramski et al., 1999, 2004;
46 Organelli et al., 2018), can serve to detect the presence of these free-living bacteria and those associated with small suspended
47 particles.

48 Time series of b_{bp} acquired by biogeochemical Argo (BGC-Argo) floats highlight the presence of a permanent layer of
49 suspended small particles in shallower oxygen-poor water masses (b_{bp} -layer) (Whitmire et al., 2009; Wojtasiewicz et al., 2018).
50 It has been hypothesized that this b_{bp} -layer is linked to N₂-yielding microbial communities such as nitrate-reducing SAR11,
51 and denitrifying, anammox, and sulphur-oxidizing bacteria. However, this hypothesis has not yet been clearly demonstrated.
52 To address this, the first step is to evaluate: (1) potential correlations between the biogeochemical factors that control the
53 presence of the b_{bp} -layer and such arrays of bacteria (O₂, NO₃⁻, OM, H₂S; Murray et al., 1995; Ward et al., 2008; Fuchsman et
54 al., 2011; Ulloa et al., 2012; Dalsgaard et al., 2014; Bristow et al., 2016), and (2) the possible relationship between the b_{bp} -
55 layer and N₂ produced by microbial communities.

56 This first step is thus essential for identifying the origin of the b_{bp} -layer and, ultimately, determining if BGC-Argo observations
57 of b_{bp} can be implemented to delineate the oxygen-poor water masses where such bacteria are confined. The Black Sea appears
58 as a suitable area for probing into the origin of the b_{bp} -layer in low-oxygen waters in this way. It is indeed a semi-enclosed
59 basin with permanently low O₂ levels where N₂ production and related nitrate-reducing SAR11, and denitrifying and anammox
60 bacteria are mainly confined within a well-defined oxygen-poor zone (Kuypers et al., 2003; Konovalov et al., 2005; Kirkpatrick
61 et al., 2012). In addition, a permanent b_{bp} -layer is a typical characteristic of this region, which is linked to such microbial
62 communities and inorganic particles (Stanev et al., 2017, 2018, see details in section 2.0).

63 The goal of our study is therefore to investigate the origin of the b_{bp} -layer in the oxygen-poor waters of the Black Sea using
64 data collected by BGC-Argo floats. More specifically, we aim to evaluate, within the oxygen-poor zone, how: (1) two of the
65 main factors (O₂ and NO₃⁻) that drive the dynamics of denitrifying and anammox bacteria, impact on the location and thickness
66 of the b_{bp} -layer, (2) NO₃⁻ controls the vertical distribution of b_{bp} within this layer, (3) temperature drives the formation of the
67 b_{bp} -layer and consumption rates of NO₃⁻, and (4) particle content inferred from b_{bp} and N₂ produced by microbial communities
68 can be at least qualitatively correlated. Ultimately, our findings allow us to infer that b_{bp} can potentially be used to detect the
69 presence of the microbial communities that drive N₂ production in oxygen-poor water masses – including nitrate-reducing
70 SAR11, and sulphur-oxidizing, denitrifying and anammox bacteria.

71 2.0. Background-nature of the small particles contributing to the b_{bp} -layer and their links with N₂ yielding

72 The oxygen-poor water masses of the Black Sea are characterized by a permanent layer of suspended small particles constituted
73 of organic and inorganic particles (Murray et al., 1995; Kuypers et al., 2003; Konovalov et al., 2005; Kirkpatrick et al., 2012).
74 In the oxygen-poor (O₂ < 3 µM) section with detectable NO₃⁻, and undetectable H₂S levels, organic particles are mainly linked

75 to microbial communities involved in the production of N₂, and these include nitrate-reducing SAR11, and anammox,
76 denitrifying, and sulphur-oxidizing bacteria (Kuypers et al., 2003; Lam et al., 2007; Yakushev et al., 2007; Fuchsman et al.,
77 2011; Kirkpatrick et al., 2012). The first group listed, SAR11, provides NO₂⁻ for N₂ yielding, and makes the largest contribution
78 (20-60%) to N₂ yielding bacteria biomass (Fuchsman et al., 2011, 2017; Tsementzi et al., 2016). Meanwhile, the second and
79 third groups of bacteria make a smaller contribution to microbial biomass (~10%; e.g. Fuchsman et al., 2011, 2017) but
80 dominate N₂ yielding via anammox (NO₂⁻ + NH₄⁺ → N₂ + 2H₂O) and heterotrophic denitrification (NO₃⁻ → NO₂⁻ → N₂O → N₂)
81 (Murray et al., 2005; Kirkpatrick et al., 2012; Devries et al., 2013; Ward, 2013). The last group can potentially produce N₂ via
82 autotrophic denitrification (e.g. 3H₂S + 4NO₃⁻ + 6OH⁻ → 3SO₄²⁻ + 2N₂ + 6H₂O; Sorokin, 2002; Konovalov et al., 2003;
83 Yakushev et al., 2007). Finally, *Epsilonproteobacteria* are the major chemoautotrophic bacteria that form organic particles in
84 the sulfidic zone (e.g. oxygen-poor section with detectable sulphide levels (> 0.3 μM) but undetectable NO₃⁻; Coban-Yildiz et
85 al., 2006; Yilmaz et al., 2006; Grote et al., 2008; Canfield and Thamdrup, 2009; Glaubitz et al., 2010; Ediger et al., 2019).
86 However, they can also be involved in the production of N₂ and linked formation of organic particles in the oxygen-poor
87 section with detectable levels of sulphide and NO₃⁻ (see Figure 1, e.g. *Epsilonproteobacteria* *Sulfurimonas* acting as an
88 autotrophic denitrifier; Glaubitz et al., 2010; Fuchsman et al., 2012b; Kirkpatrick et al., 2018)

89 The inorganic component is mainly due to sinking particles of manganese oxides (Mn, III, IV) that are formed due to the
90 oxidation of dissolved Mn (II, III) pumped from the sulfidic zone (e.g. 2Mn²⁺(l) + O₂ + 2H₂O → 2MnO₂(s) + 4H⁺; Konovalov
91 et al., 2003; Clement et al., 2009; Dellwig et al., 2010). Ultimately, sinking particles of manganese oxides are dissolved back
92 to Mn (II, III), mainly via chemosynthetic bacteria that drive sulphur reduction (e.g. HS⁻ + MnO₂(s) + 3H⁺ → S⁰ + Mn²⁺(l) +
93 2H₂O; Jorgensen et al., 1991; Konovalov et al., 2003; Johnson, 2006; Yakushev et al., 2007; Fuchsman et al., 2011; Stanev et
94 al., 2018). Overall, these arrays of bacteria mediate the reactions described above by using electron acceptors according to the
95 theoretical “electron tower” (e.g., O₂ → NO₃⁻ → Mn(IV) → Fe(III) → SO₄²⁻; Stumm and Morgan, 1970; Murray et al., 1995;
96 Canfield and Thamdrup, 2009). Therefore, the vertical distributions of NO₃⁻, N₂ excess, and content of small particles are
97 driven by the reactions that occur in the chemical zones of oxygen-poor water masses (e.g. nitrogenous and manganous zones,
98 which correspond to the sections where NO₃⁻ and Mn(IV), respectively, are predominantly used as electron acceptors; Murray
99 et al., 1995; Konovalov et al., 2003; Yakushev et al., 2007; Canfield and Thamdrup, 2009; see also sections 4.2 and 4.3).

100 3 Methods

101 3.1 Bio-optical and physicochemical data measured by BGC-Argo floats

102 We used data collected by three BGC-Argo floats that profiled at a temporal resolution of 5-10 days in the first 1000 m depth
103 of the Black Sea from December 2013 to July 2019 (Figure 1). These floats — allocated the World Meteorological
104 Organization (WMO) numbers 6900807, 6901866, and 7900591 — collected 239, 301, and 518 vertical profiles, respectively.
105 BGC-Argo float 6901866 was equipped with four sensors: (1) a SBE-41 CP conductivity-T-depth sensor (Sea-Bird Scientific),
106 (2) an Aanderaa 4330 optode (serial number:1411; O₂ range: 0-1000 μM, with an accuracy of 1.5%), (3) a WETLabs ECO
107 Triplet Puck, and (4) a Satlantic Submersible Ultraviolet Nitrate Analyzer (SUNA). These sensors measured upward profiles
108 of: (1) temperature (T), conductivity, and depth, (2) dissolved oxygen (O₂), (3) chlorophyll fluorescence, total optical
109 backscattering (particles + pure seawater) at 700 nm and fluorescence by Colored Dissolved Organic Matter, and (4) nitrate
110 (NO₃⁻; detection limit of ~0.5 μM with T/salinity correction processing) and bisulfide (HS⁻, detection limit of ~0.5 μM; Stanev
111 et al., 2018). Floats 6900807 and 7900591 were equipped with only the first three sensors.

112 Raw data of fluorescence and total backscattering were converted into Chlorophyll concentration (*chl*) and particle
113 backscattering (*b_{bp}*) following standard protocols, **respectively** (Schmechtig et al., 2014, 2015). Spike signals in vertical
114 profiles of *chl* and *b_{bp}* and due to particle aggregates were removed by using a median filter with a window size of three data
115 points (Briggs et al., 2011). NO₃⁻, HS⁻ and O₂ data were processed following BGC-Argo protocols (**Bittig and Körtzinger,**
116 **2015**; Johnson et al., 2018; Thierry et al., 2018). Sampling regions covered by the three floats encompassed most of the Black
117 Sea area (Figure 1, and Appendix A). However, we only used data collected during periods without a clear injection of small
118 particles derived from the productive layer and Bosphorus plume (e.g. advection of water masses, Stanev et al., 2017). This
119 restriction allowed us to focus on the *in-situ* 1D processes driving local formation of the *b_{bp}-layer*, with minimal interference
120 from any possible external sources of small particles.

121 We only describe the time series of data collected by float 6901866 because this was the only float carrying a NO₃⁻/HS⁻ sensor.
122 Data acquired by floats 6900807 and 7900591 are described in Appendix A, and nevertheless used as complementary data to
123 those of float 6901866 to corroborate: (1) qualitative correlations between O₂ levels and the location of the *b_{bp}-layer*, and (2)
124 consistency in the location of the *b_{bp}* maximum within the *b_{bp}-layer*.

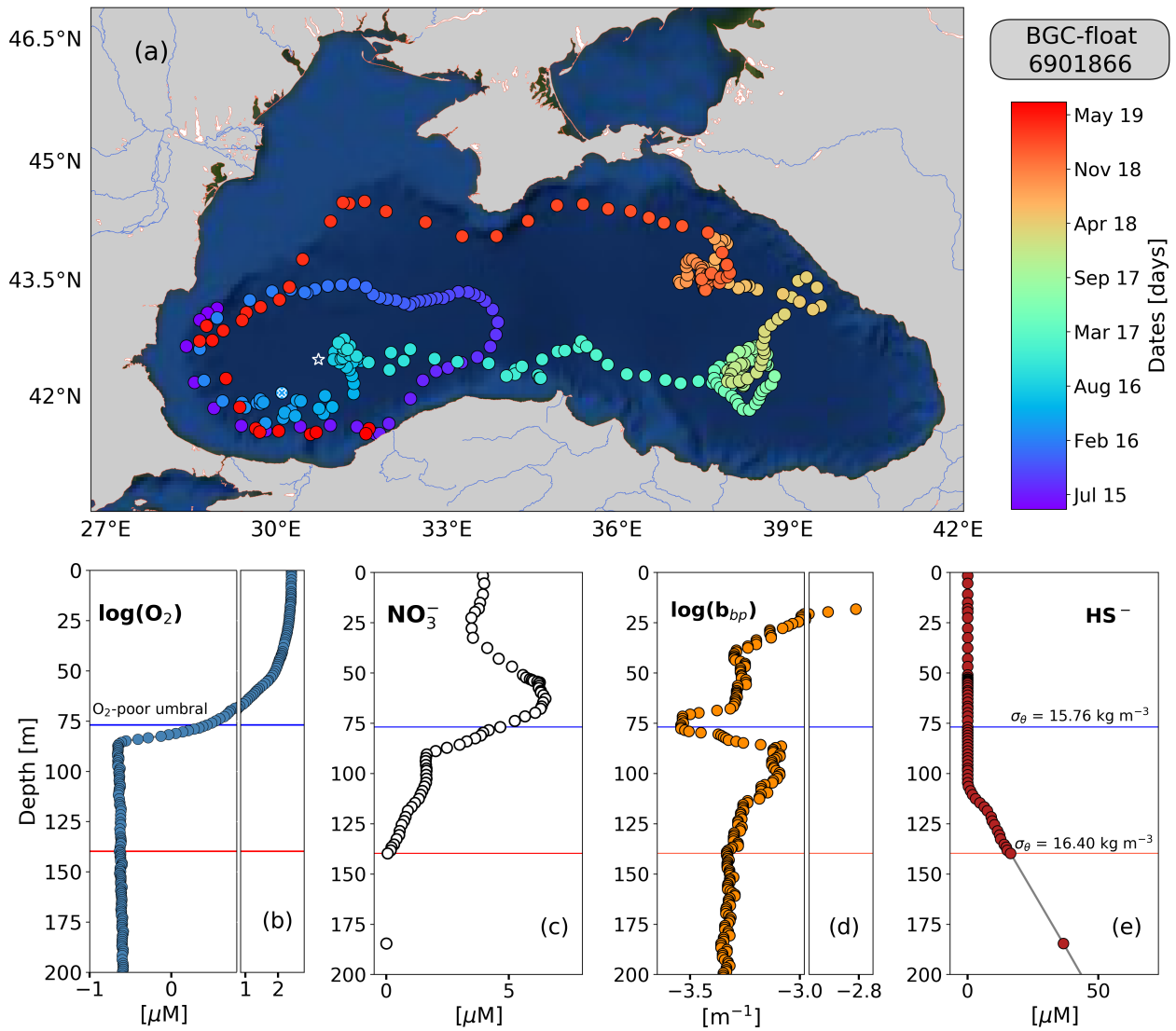
125 **3.2 Defining the oxygen-poor zone, mixed layer depth, and productive layer**

126 We used O₂ and NO₃⁻ to respectively define the top and bottom isopycnals of the **oxygen-poor zone** where denitrifying and
127 anammox bacteria are expected to be found. To set the top isopycnal, we applied an O₂ threshold of ~3 μM because denitrifying
128 and anammox bacteria seem to tolerate O₂ concentrations beneath this threshold (Jensen et al., 2008; **Dalsgaard et al., 2014**;
129 **Babbin et al., 2014**). The bottom isopycnal was defined as the deepest isopycnal at which NO₃⁻ was detected by the SUNA
130 sensor (0.23 ± 0.32 μM). NO₃⁻ was used to set this isopycnal because heterotrophic denitrification and subsequent reactions
131 cannot occur without NO₃⁻ (Lam et al., 2009; Bristow et al., 2017). HS⁻ was not used to delimit the bottom of this zone because
132 the maximum concentration of **HS** that denitrifying and anammox bacteria tolerate is not well established (Murray et al., 1995;
133 Kirkpatrick et al., 2012; see also section 4.1).

134 Mixed layer depth (MLD) was computed as the depth at which density differed from 0.03 kg m⁻³ with respect to the density
135 recorded at 1m depth (de Boyer Montégut et al., 2004). We used *chl* to define the productive layer where living phytoplankton
136 were present and producing particulate organic carbon. The base of this layer was set as the depth at which *chl* decreased
137 below 0.25 mg m⁻³. This depth was used only as a reference to highlight the periods when surface-derived small particles were
138 clearly injected into the **oxygen-poor** zone.

139 **3.3 Complementary cruise data on N₂ excess and NO₃⁻**

140 Published data on N₂:Ar ratios and NO₃⁻ collected at the southwest of the Black Sea in March 2005 (Fuchsman et al., 2008,
141 2019) were exploited to complement discussion of our results. N₂ produced by anaerobic microbial communities (N₂ excess,
142 μM) was estimated from N₂:Ar ratios and argon concentrations at atmospheric saturation (Hamme and Emerson, 2004). N₂
143 excess data were used to: (1) describe the **oxygen-poor** zone where N₂ is expected to be predominantly produced, and (2)
144 highlight qualitative correlations between N₂ excess, the location of the *b_{bp}-layer*, and vertical distribution of small particles
145 within the *b_{bp}-layer*.



146

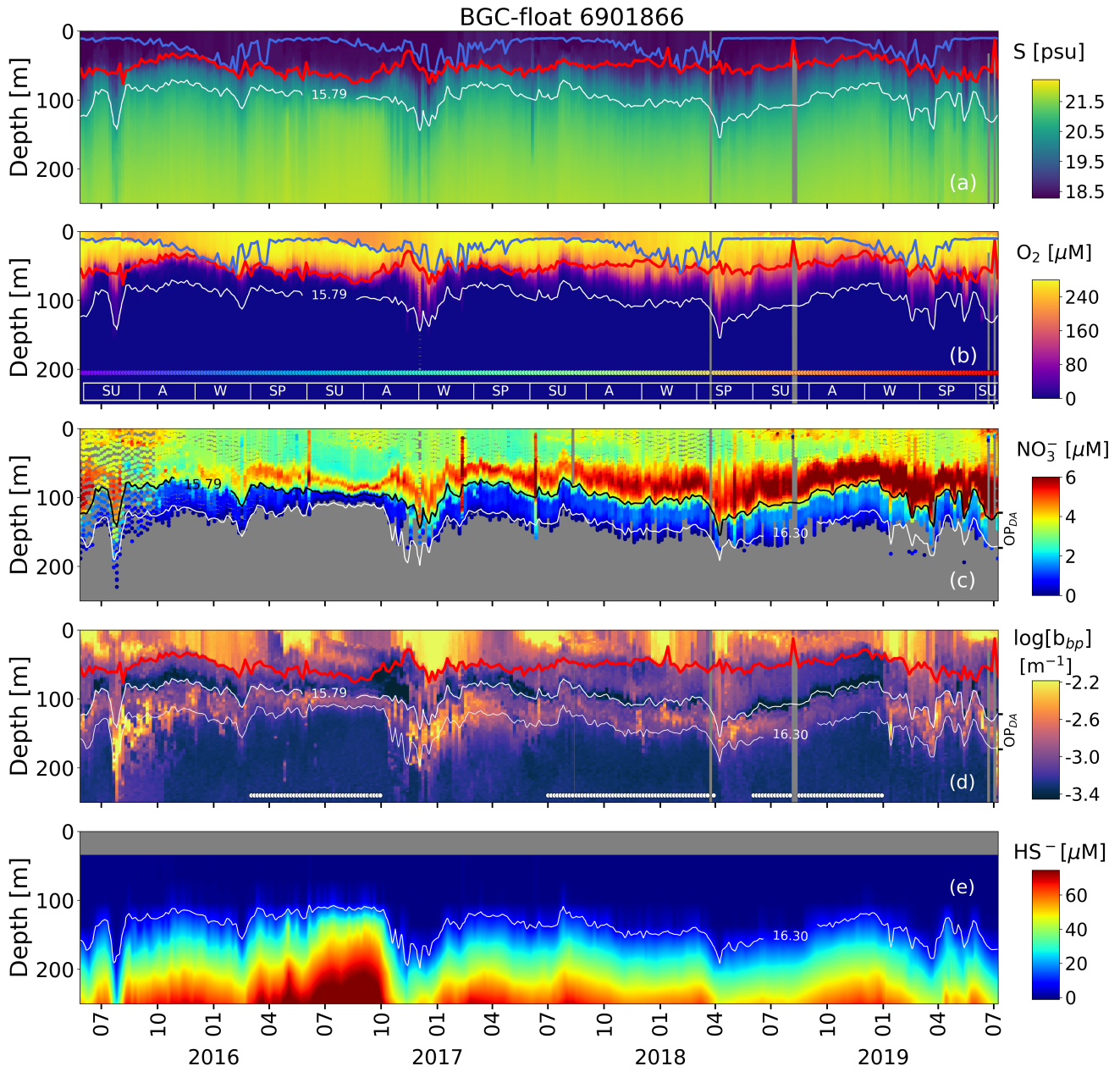
147 **Figure 1: (a) Sampling locations of float 6901866 between May 2015 and July 2019. Colored circles indicate the date**
 148 **(color bar) for a given profile. The white star in (a) marks the sampling site of the cruise (March 2005). The white x in**
 149 **(a) highlights the float location on 6th April 2016. Float profiles of (b) log(O₂), (c) NO₃⁻, (d) log(b_{bp}), and (e) HS⁻ collected**
 150 **on 24th November 2018.**

151 **4 Results and discussion**

152 **4.1 Description of the oxygen-poor zone**

153 The top and bottom of the oxygen-poor zone are located around the isopycnals (mean ± standard deviation) $15.79 \pm 0.23 \text{ kg m}^{-3}$
 154 m^{-3} and $16.30 \pm 0.09 \text{ kg m}^{-3}$, respectively. The two isopycnals therefore delimit the oxygen-poor water masses where nitrate-
 155 reducing SAR11, and denitrifying, anammox, and sulphur-oxidizing bacteria are expected to be found (zone hereafter called
 156 the $OP_{D,A}$, Figure 2; Kuypers et al., 2003; Lam et al., 2007; Yakushev et al., 2007; Fuschman et al., 2011; Kirkpatrick et al.,
 157 2012). The top location of the $OP_{D,A}$ shows large spatial-temporal variability ranging between 80-180 m (or σ_θ between 15.5-
 158 15.9 kg m^{-3} , Figure 2). Similarly, the $OP_{D,A}$ thickness varies between 30-80 m, which corresponds to a σ_θ separation of ~ 0.50
 159 kg m^{-3} . The bottom of the $OP_{D,A}$ is slightly sulfidic ($\text{HS}^- = 11.4 \pm 3.53 \text{ } \mu\text{M}$, $n = 86$) and deeper than suggested (e.g. $\sigma_\theta = 16.20$

160 kg m⁻³, and H₂S ≤ 10 nM, Murray et al., 1995). However, our results coincide with the slightly sulfidic conditions of the deepest
 161 isopycnal at which anammox bacteria can be still recorded (σ_{θ} = 16.30 kg m⁻³, and H₂S ≥ 10 μM; Kirkpatrick et al., 2012).



162
 163 **Figure 2: Time series of: (a) Salinity (S), (b) O₂, (c) NO₃⁻, (d) log(*b_{bp}*), and (e) HS⁻. The blue lines in (a) and (b) indicate**
 164 **the mixed layer depth. The red lines in (a), (b) and (d) show the base of the productive region. The isopycnals 15.79 kg**
 165 **m⁻³ and 16.30 kg m⁻³ describe the top and bottom of the oxygen-poor zone (*OP_{D-A}*), respectively. SU, A, W, and SP stand**
 166 **for summer, autumn, winter, and spring, respectively. The colored horizontal line in (b) indicates the sampling site for**
 167 **a given date (Figure 1). The horizontal white lines in (d) are the profiles used to: (1) delimit the *OP_{D-A}*, and (2) compute**
 168 **correlations between *b_{bp}*, NO₃⁻, and T within the *OP_{D-A}*.**

169 **4.2 NO₃⁻, O₂, and MnO₂ as key drivers of the thickness and location of the suspended small-particle layer**

170 The permanent *b_{bp}*-layer is always confined within the two isopycnals that delimit the *OP_{D-A}* (Figure 2). It follows that the
 171 thickness and top location of this layer demonstrate the same spatial and temporal variability as the one described for the *OP_D*

172 (Figure 2 and Appendix A). This correlation indicates that variations in the thickness and top location of the b_{bp} -layer are
173 partially driven, respectively, by: (1) the amount of NO_3^- available to produce N_2 inside the $OP_{D,A}$ via the set of bacteria
174 communities involved, and (2) downward ventilation of oxygen-rich subsurface waters (Figure 2 and Appendix A).

175 NO_3^- and O_2 are two of the key factors that modulate the presence of: (1) denitrifying and anammox bacteria working in
176 conjunction with nitrate-reducing SAR11 (Fuschman et al., 2011; Ulloa et al., 2012; Tsementezi et al., 2016; Bristow et al.,
177 2017), and probably with chemoautotrophic ammonia-oxidizing bacteria (in this case, only with anammox, e.g. γ AOB; Ward
178 and Kilpatrick, 1991; Lam et al., 2007), and (2) sulphur-oxidizing bacteria (e.g. SUP05 and potentially *Epsilonproteobacteria*
179 *Sulfurimonas*; Canfield et al., 2010; Glaubitz et al., 2010; Fuschman et al., 2011, 2012b; Ulloa et al., 2012; Kirkpatrick et al.,
180 2018). Therefore, the results described above highlight that at least a fraction of the b_{bp} -layer should be due to this array of
181 bacteria. This notion is supported by three main observations. Firstly, the top location of the b_{bp} -layer is driven by the intrusion
182 of subsurface water masses ($S \leq 20.36 \pm 0.18$ psu) with O_2 concentrations above the levels tolerated by denitrifying and
183 anammox bacteria ($\text{O}_2 \geq 3 \mu\text{M}$, Jensen et al., 2008; Babbitt et al., 2014; Figure 2). As a result, in regions where O_2 is ventilated
184 to deeper water masses, the top location of the b_{bp} -layer is also deeper. The contrary is observed when O_2 ventilation is
185 shallower (Figure 2 and Appendix A). Secondly, nitrate-reducing SAR11, and denitrifying, anammox, and sulphur-oxidizing
186 bacteria reside between the isopycnals $15.60\text{-}16.30 \text{ kg m}^{-3}$ (Fuschman et al., 2011; 2012a; Kirkpatrick et al., 2012), while the
187 b_{bp} -layer is formed between isopycnals $\sim 15.79\text{-}16.30 \text{ kg m}^{-3}$. We can thus infer coexistence of such bacteria between the
188 coincident isopycnals where the b_{bp} -layer is generated. Thirdly, NO_3^- declines from around isopycnal 15.79 kg m^{-3} to the
189 isopycnal 16.30 kg m^{-3} due to the expected N_2 production via the microbial communities involved (Figures 2-3, and Kirkpatrick
190 et al., 2012).

191 The ventilation of subsurface O_2 is also key in driving the depth at which MnO_2 is formed ($\text{O}_2 \leq 3\text{-}5 \mu\text{M}$; Clement et al., 2009),
192 and can thus contribute to setting the characteristics of the b_{bp} -layer via its subsequent accumulation and dissolution
193 (Konovalov et al., 2003; Clement et al., 2009; Dellwig et al., 2010). Thus, in regions where subsurface O_2 (e.g. $\text{O}_2 \geq 3\text{-}5 \mu\text{M}$,
194 and $S \leq 20.36 \pm 0.18$ psu) is ventilated to deeper water masses, both the formation of MnO_2 and top location of the b_{bp} -layer
195 can be expected to be deeper, and vice versa (Figure 2). Finally, the dissolution of MnO_2 should also influence the thickness
196 of the b_{bp} -layer because it occurs just beneath the maxima of the optical particles inside this layer (Konovalov et al., 2006; see
197 the explanation in section 4.3).

198 Overall, the qualitative evidence presented above points out that particles of MnO_2 as well as nitrate-reducing SAR11, and
199 denitrifying, anammox, and sulphur-oxidizing bacteria, appear to define the characteristics of the b_{bp} -layer (Johnson, 2006;
200 Konovalov et al., 2003; Fuschman et al., 2011, 2012b; Stanev et al., 2018). This observation leads us to argue, in the next
201 section, that the b_{bp} -layer is partially composed of the main group of microbial communities involved in N_2 yielding, as well
202 as of MnO_2 .

203 4.3 Role of the removal rate of NO_3^- , MnO_2 , and temperature in the vertical distribution of small particles

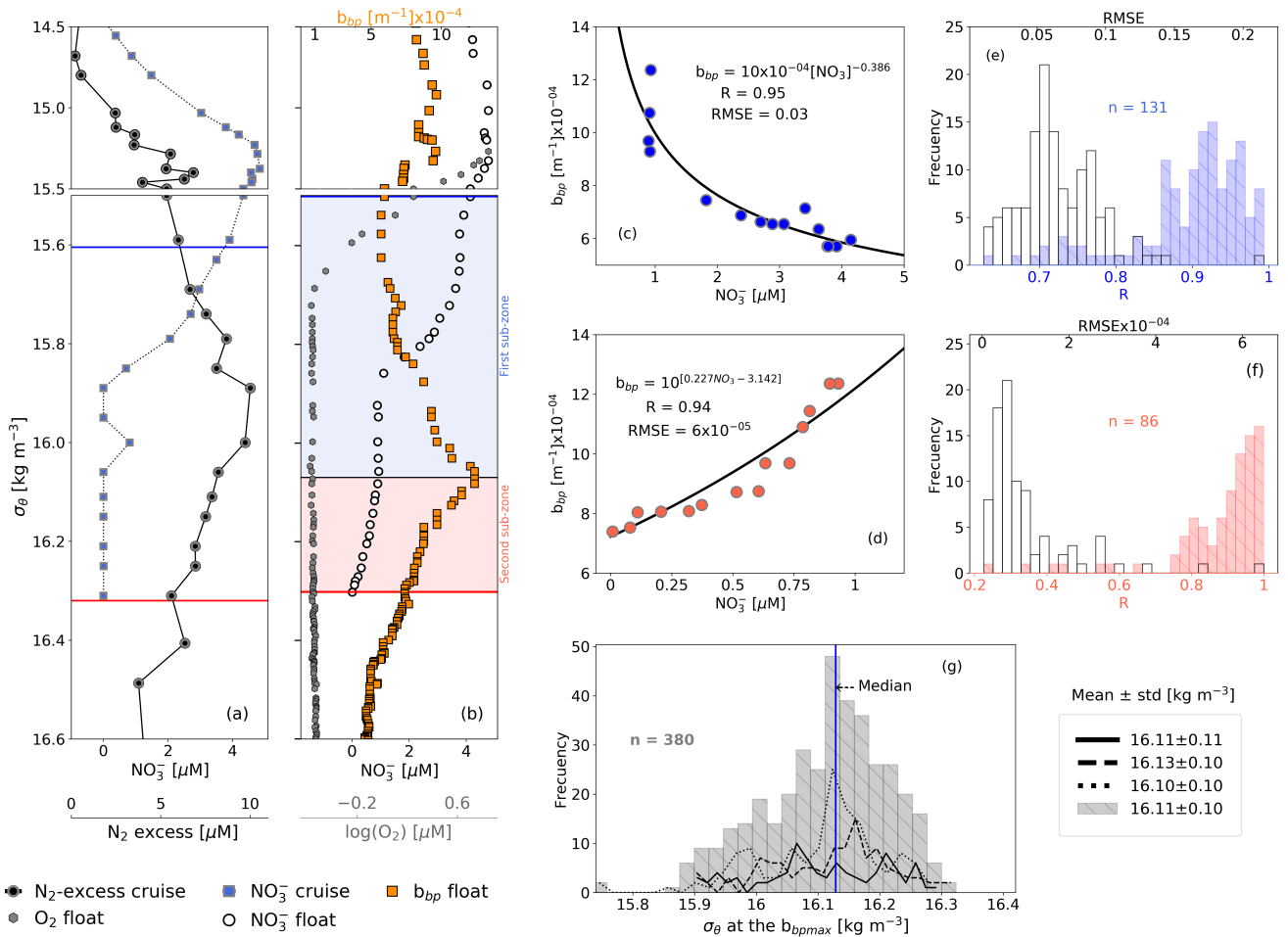
204 We propose that the removal rate of NO_3^- is a key driver of the vertical distribution of small particles and N_2 excess within the
205 $OP_{D,A}$. This is because the vertical profiles of small particles and of N_2 excess are qualitatively similar, and both profiles are
206 clearly related to the rate at which NO_3^- is removed from the $OP_{D,A}$ (Figures 3-4). For instance, maxima of N_2 excess and b_{bp}
207 coincide around the isopycnal $16.11 \pm 0.11 \text{ kg m}^{-3}$ (Figure 3; Konovalov et al., 2005; Fuschman et al., 2008, 2019). At this
208 isopycnal, the mean concentration of NO_3^- is $1.19 \pm 0.53 \mu\text{M}$. We thus propose that this NO_3^- threshold value splits the $OP_{D,A}$
209 in two sub-zones with distinctive biogeochemical conditions (e.g. nitrogenous and manganous zones; Canfield and Thamdrup,

210 2009). Ultimately, these two different sets of conditions drive the rates at which NO_3^- and small particles are removed and
211 formed within the OP_{D-A} , respectively (Figure 3, and explanation below).

212 The first sub-zone is thus located between the top of the OP_{D-A} ($\sigma_\theta = 15.79 \text{ kg m}^{-3}$) and around the isopycnal 16.11 kg m^{-3} .
213 Here, removal rates of NO_3^- ($-0.16 \pm 0.10 \text{ } \mu\text{M m}^{-1}$, Figure 4) are likely to be boosted by: (1) high content of organic matter
214 (dissolved organic carbon = $122 \pm 9 \text{ } \mu\text{M}$, Margolin et al., 2016) and NO_3^- ($\geq 1.19 \pm 0.53 \text{ } \mu\text{M}$), and (2) O_2 levels staying between
215 a range that maintain the yielding of N_2 ($0.24 \pm 0.04 \text{ } \mu\text{M} \geq \text{O}_2 \leq 2.8 \pm 0.14 \text{ } \mu\text{M}$, $n = 100$, the means of the minima and maxima
216 of O_2 , respectively, in the first sub-zone) and promote the formation of MnO_2 (e.g. maximum of Mn(II) oxidation is at O_2 levels
217 $\sim 0.2 \text{ } \mu\text{M}$; Clement et al., 2009). Consequently, the formation of biogenic and inorganic small particles (and related N_2 excess)
218 increases from the top of the OP_{D-A} to around the isopycnal 16.11 kg m^{-3} (Figure 3). This hypothesis is: (1) in part confirmed
219 by significant and negative power-law correlations between the suspended small-particle content and NO_3^- in this sub-zone
220 (Figure 3), and (2) in agreement with the progressive accumulation of MnO_2 from around isopycnal 15.8 kg m^{-3} to the isopycnal
221 16.10 kg m^{-3} (e.g. Konovalov et al., 2006).

222 The second sub-zone is located between isopycnal 16.11 kg m^{-3} and the bottom of the OP_{D-A} ($\sigma_\theta = 16.30 \text{ kg m}^{-3}$, Figure 3).
223 Here, NO_3^- is low ($\leq 1.19 \pm 0.53 \text{ } \mu\text{M}$) and O_2 is relatively constant ($0.23 \pm 0.02 \text{ } \mu\text{M}$, $n = 2284$, mean of O_2 calculated in the
224 second sub-zone for all profiles), or lower than the minimum of O_2 recorded by this sensor ($0.22 \pm 0.02 \text{ } \mu\text{M}$, $n = 89$). These
225 constant (or lower) levels of O_2 roughly correspond to those at which anammox and heterotrophic denitrification are inhibited
226 by $\sim 50\%$ ($0.21 \text{ } \mu\text{M}$, and $0.81 \text{ } \mu\text{M}$, respectively; Dalsgaard et al., 2014). In addition, low levels of NO_3^- necessarily promotes
227 the microbial use of Mn(IV) as an electron acceptor, ultimately dissolving the particles of MnO_2 into Mn(II) (e.g. manganous
228 zone; Konovalov et al., 2006; Yakushev et al., 2007; Canfield and Thamdrup, 2009). As a result, this sub-zone exhibits a
229 decline in removal rates of NO_3^- ($-0.04 \pm 0.01 \text{ } \mu\text{M m}^{-1}$, Figure 4) along with inhibited formation of biogenic small particles and
230 dissolution of MnO_2 . Ultimately, both the content of small particles and related N_2 excess decrease from around isopycnal
231 16.11 kg m^{-3} to the bottom of the OP_{D-A} (Figure 3). These results are in agreement with: (1) significant and positive exponential
232 correlations computed between the small-particle content inferred from b_{bp} and NO_3^- within this sub-zone (Figure 3), and (2)
233 the overlap of nitrogenous and manganous zones in this sub-zone because the content of MnO_2 particles and dissolved Mn(II)
234 concurrently declines and increases just beneath the isopycnal 16.11 kg m^{-3} , respectively (e.g. Murray et al., 1995; Konovalov
235 et al., 2003, 2005, 2006; Yakushev et al., 2007; Canfield and Thamdrup, 2009).

236 Strong-positive linear correlations are also recorded between b_{bp} and T in the first sub-zone of the OP_{D-A} (Figure 4). This is
237 likely to indicate that the formation of small particles is sensitive to very tiny increments in T ($0.003 \pm 0.001 \text{ } ^\circ\text{C m}^{-1}$, $n = 133$).
238 We thus infer a tendency for the decline rates of NO_3^- and related production of N_2 to increase with T. This hypothesis is at
239 least partially supported by the significant correlation between NO_3^- decline rates and T increase rates in this sub-zone (Figure
240 4). Within the second sub-zone, T continues increasing while b_{bp} decreases, likely due to inhibition of the formation of small
241 particles for the reasons described above (Figure 4). These observations suggest that the production of small particles is likely
242 to have first- and second-order covariations, with NO_3^- and T, respectively — a likelihood backed up by a lack of correlation
243 between NO_3^- decline rates and T increase rates in this sub-zone (Figure 4). Finally, more information is needed to investigate
244 the physical and/or biogeochemical processes driving the correlation between the increase rates of T, and declines rates of
245 NO_3^- in the first sub-zone. This is however out of the scope of our study.



246

247

248

249

250

251

252

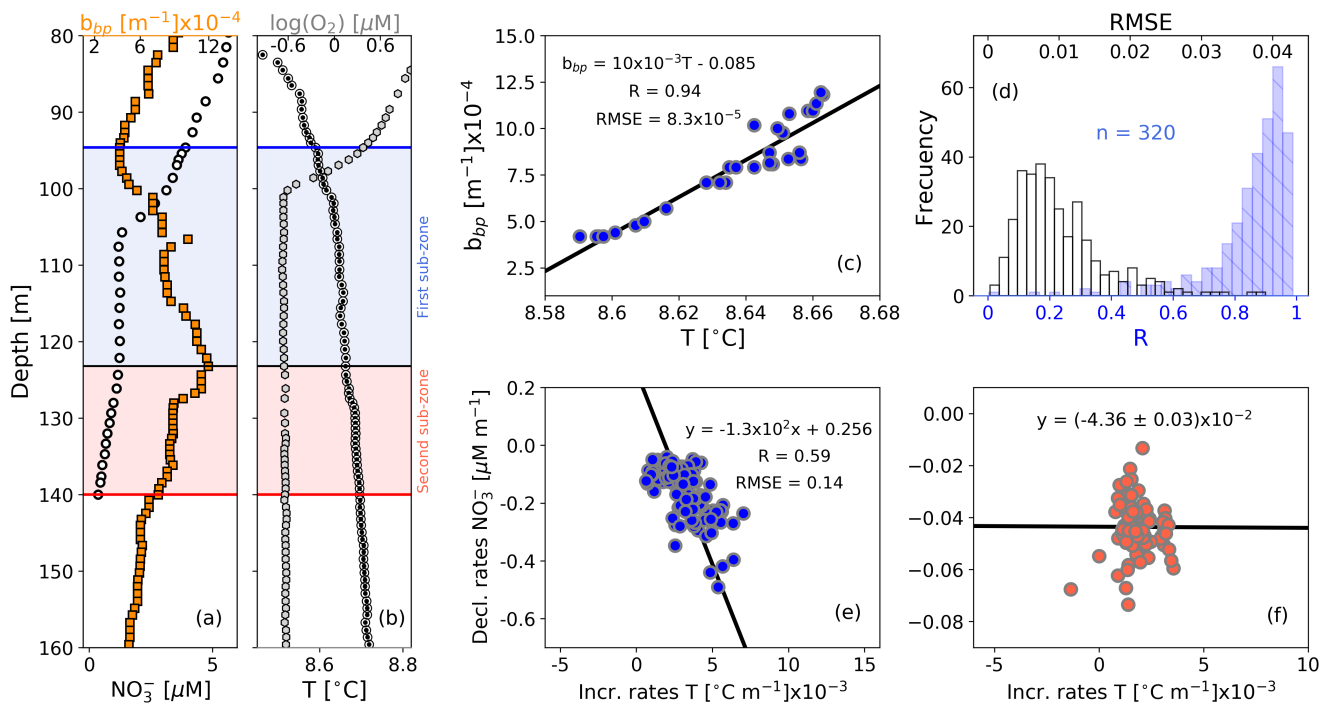
253

254

255

256

Figure 3: (a) Cruise profiles of NO_3^- , and N_2 excess, collected in March 2005 (Fuchsman et al., 2019). (b) Float profiles of NO_3^- , b_{bp} , and $\log(\text{O}_2)$ measured on 6th April 2016. Profiles in (a) and (b) were conducted at the northwest of the basin (see Figure 1). The top and bottom of the $OP_{D_{2A}}$ are described in (a) and (b) as horizontal blue and red lines, respectively. The b_{bp} maximum is the horizontal black line in (b). The first and second sub-zone of the $OP_{D_{2A}}$ are respectively highlighted in (b) as blue and red squares. NO_3^- vs b_{bp} in (c) the first, and (d) the second sub-zone, of the float profile in (b). The number of data points visualized in (c) is lower than in (b) for the first sub-zone because b_{bp} and NO_3^- are not always recorded at the same depths. (e) Frequency distributions of correlation coefficients (R, blue bars), and root mean square errors (RMSE, white bars) for NO_3^- vs b_{bp} in the first sub-zone. (f) Same as (e) but for the second sub-zone. (g) Frequency distributions of the isopycnals at which b_{bp} maxima are found within the $OP_{D_{2A}}$. Dotted, dashed, and solid black lines in (g) are data collected by floats 7900591, 6901866, and 6900807, respectively. Gray bars include all data.



257
 258 **Figure 4: Float profiles of (a) NO_3^- , and b_{bp} , and (b) T and $\log(\text{O}_2)$ collected on 10th September 2017. Horizontal blue**
 259 **and red lines in (a) and (b) are the top and bottom of the OP_{D-2} . The b_{bp} maximum is indicated in (a) and (b) as horizontal**
 260 **black lines. The first and second sub-zones of the OP_{D-2} are respectively highlighted in (a) and (b) as blue and red**
 261 **squares. (c) b_{bp} vs T for the first sub-zone of the profile in (b). (d) Frequency distributions of correlation coefficients (R,**
 262 **blue bars), and root mean square errors (RMSE, white bars), for b_{bp} vs T in the first sub-zone, including data collected**
 263 **by the three floats. Decrease rates of NO_3^- vs increase rates of T in (e) the first and (f) the second sub-zone.**

264 To summarize, BGC-Argo float data combined with a proxy of N_2 production suggest that in regions without the Bosphorus
 265 plume influence, the b_{bp} -layer systematically tracks and delineates the effective N_2 -yielding section independently of: (1) the
 266 biogeochemical mechanisms driving N_2 yielding, and (2) the contribution that MnO_2 and other microorganisms can be
 267 expected to make to the formation of the b_{bp} -layer (e.g. Lam et al., 2007; Fuchsman et al., 2011; 2012a; Kirkpatrick et al.,
 268 2018). It is thus finally inferred that this b_{bp} -layer is at least partially composed of the predominant anaerobic microbial
 269 communities involved in the production of N_2 , such as nitrate-reducing SAR11, and anammox, denitrifying, and sulphur-
 270 oxidizing bacteria. These results also suggest that N_2 production rates can be highly variable in the Black Sea because the
 271 characteristics of the b_{bp} -layer show large spatial-temporal variations driven by changes in NO_3^- and O_2 (Figures 2 and 4).
 272 Finally, we propose that b_{bp} and O_2 can be exploited as a combined proxy for defining the N_2 -producing section of the oxygen-
 273 poor Black Sea. We consider that this combined proxy can delineate the top and base of this section, by applying an O_2
 274 threshold of $3.0 \mu\text{M}$, and the bottom isopycnal of the b_{bp} -layer, respectively. This section should thus be linked to free-living
 275 bacteria ($0.2\text{-}2 \mu\text{m}$), and those associated with small suspended particles ($> 2\text{-}20 \mu\text{m}$), as well as to small inorganic particles
 276 ($0.2\text{-}20 \mu\text{m}$).

277 4.4 New perspectives for studying N_2 losses in ODZs

278 The conclusions and inferences of this study, especially those related to the origin and drivers of the b_{bp} -layer, primarily apply
 279 to the Black Sea. However, these findings may also have a wider application. In particular, the shallower water masses of
 280 oxygen-deficient zones (ODZs) are similarly characterized by the formation of a layer of suspended small particles that can

281 be optically detected by b_{bp} and the attenuation coefficients of particles (Spinrad et al., 1989; Naqvi et al., 1993; Whitmire et
282 al., 2009). This layer is **mainly** linked to N_2 -yielding microbial communities because: **(1)** its location coincides with the maxima
283 of N_2 excess, microbial metabolic activity, and nitrite (NO_2^- , the intermediate product of denitrification-anammox that is mainly
284 accumulated in the N_2 -yielding section, Spinrad et al., 1989; Naqvi et al., 1991, 1993; Devon et al., 2006; Chang et al., 2010,
285 2012; Ulloa et al., 2012; Wojtasiewicz et al., 2018), **and (2) MnO_2 is not accumulated as in the Black Sea (Martin and Knauer,
286 1984; Johnson et al., 1996; Lewis and Luther, 2000).** Therefore, our findings suggest that highly resolved vertical profiles of
287 b_{bp} and O_2 can potentially be used as a combined proxy to define the *effective* N_2 -production section of ODZs. Such definition
288 can be key to better-constrained global estimates of N_2 loss rates because it can allow us to: (1) accurately predict the **oxygen-**
289 **poor** water volume where around 90% of N_2 is produced in the ODZ core (Babin et al., 2014), and (2) evaluate how the location
290 and thickness of the N_2 -yielding section vary due to changes in the biogeochemical factors that modulate anammox and
291 heterotrophy denitrification.

292 Global estimates of N_2 losses differ by 2-3 fold between studies (e.g. 50-150 Tg $N\ yr^{-1}$, Codispoti et al., 2001; Bianchi et al.,
293 2012, 2018; DeVries et al., 2012; Wang et al., 2019). These discrepancies are caused in part by inaccurate estimations of the
294 **oxygen-poor** volume of the N_2 -production section. Other sources of uncertainties arise from the methods applied to estimate
295 the amount of POC that fuels N_2 production. For instance, POC fluxes and their subsequent attenuation rates are not well
296 resolved because they are computed respectively from satellite-based primary-production algorithms and generic power-law
297 functions (Bianchi et al., 2012, 2018; DeVries et al., 2012). POC-flux estimates based on these algorithms visibly exclude: (1)
298 POC supplied by zooplankton migration (Kiko et al., 2017; Tutasi and Escibano, 2020), (2) substantial events of POC export
299 decoupled from primary production (Karl et al., 2012), and (3) the role of small particles derived from the physical and
300 biological fragmentation of larger ones (Karl et al., 1988; Briggs et al., 2020), **which are more efficiently remineralized by**
301 **bacteria in ODZs (Cavan et al., 2017).** In addition, these estimates do not take into consideration the inhibition effect that O_2
302 intrusions may have on N_2 -yield rates (Whitmire et al., 2009; Ulloa et al., 2012; Dalsgaard et al., 2014; Peters et al., 2016;
303 Margolskee et al., 2019).

304 Overall, mechanistic predictions of N_2 losses misrepresent the strong dynamics of the biogeochemical and physical processes
305 that regulate them. Consequently, it is still debated whether the oceanic nitrogen cycle is in balance or not (Codispoti, 2007;
306 Gruber and Galloway, 2008; DeVries et al., 2012; Jayakumar et al., 2017; Bianchi et al., 2018; Wang et al., 2019). The
307 subsiding uncertainty points to a compelling need for alternative methods that allow accurate refinement of oceanic estimations
308 of N_2 losses.

309 Our study supports the proposition that robotic observations of b_{bp} and O_2 can be used to better delineate the N_2 -yielding section
310 at the appropriate spatial (e.g. vertical and regional) and temporal (e.g. event, seasonal, interannual) resolutions. In addition,
311 POC fluxes **and N_2** can be simultaneously quantified using the same float technology (BGC-Argo, Bishop et al., 2009;
312 Dall'Olmo and Mork, 2014; Reed et al., 2018; Boyd et al., 2019; Estapa et al., 2019; Rasse and Dall'Olmo, 2019). These
313 robotic measurements can contribute to refining global estimates of N_2 losses by better constraining both the **oxygen-poor**
314 **section** where N_2 is produced, and POC fluxes that fuel its loss. Ultimately, O_2 intrusions into the N_2 -yielding section can
315 potentially be quantified by BGC-Argo floats to assess their regulatory effect on N_2 losses.

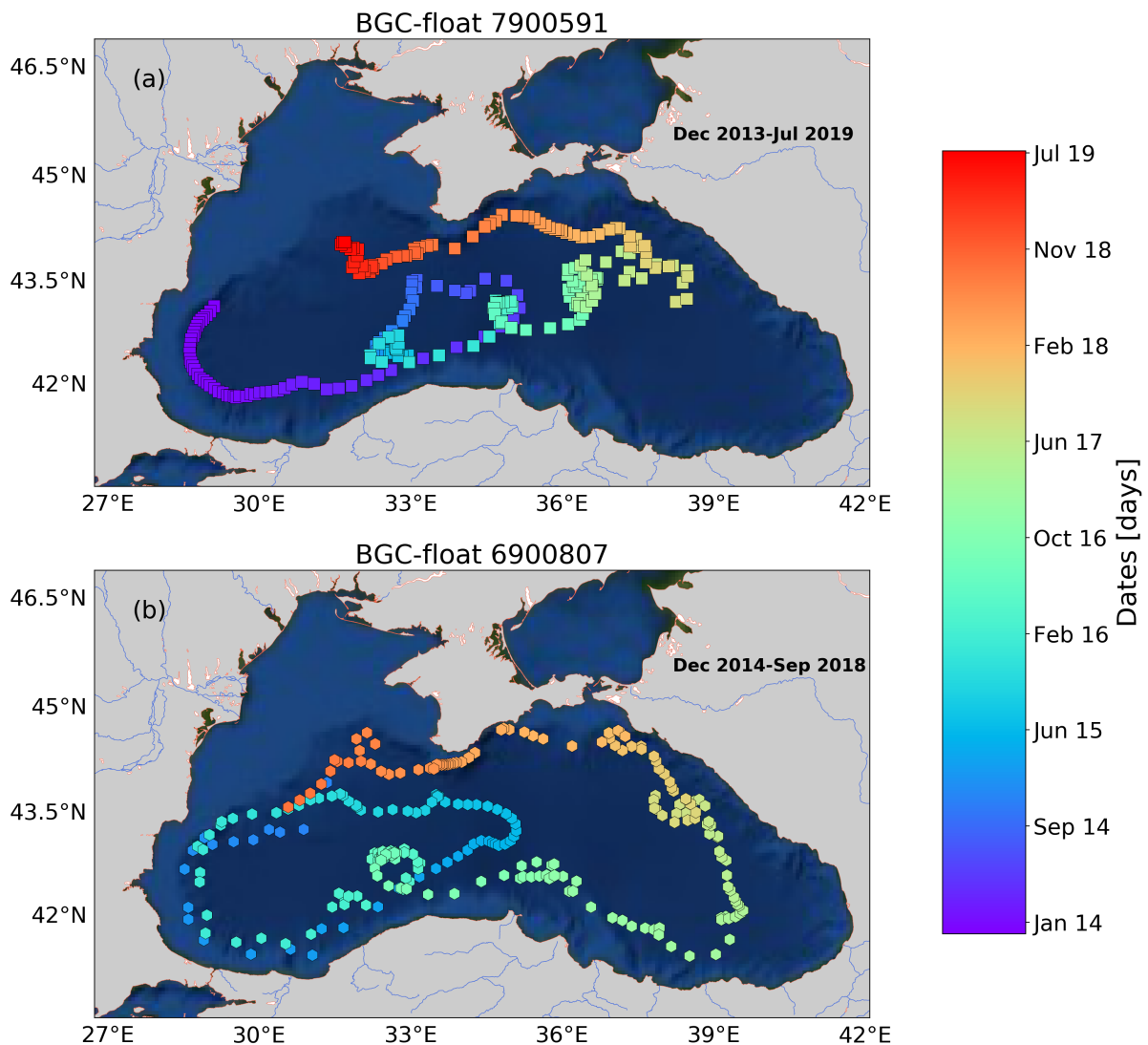
316 **Conclusions**

317 **Our results along with those from previous studies suggest** that the b_{bp} -layer of the **oxygen-poor** Black Sea is at least partially
318 composed of **nitrate-reducing SAR11, and anammox, denitrifying, and sulphur-oxidizing bacteria.** The location and thickness
319 of this layer show strong spatial-temporal variability, mainly driven by the ventilation of oxygen-rich subsurface waters, and

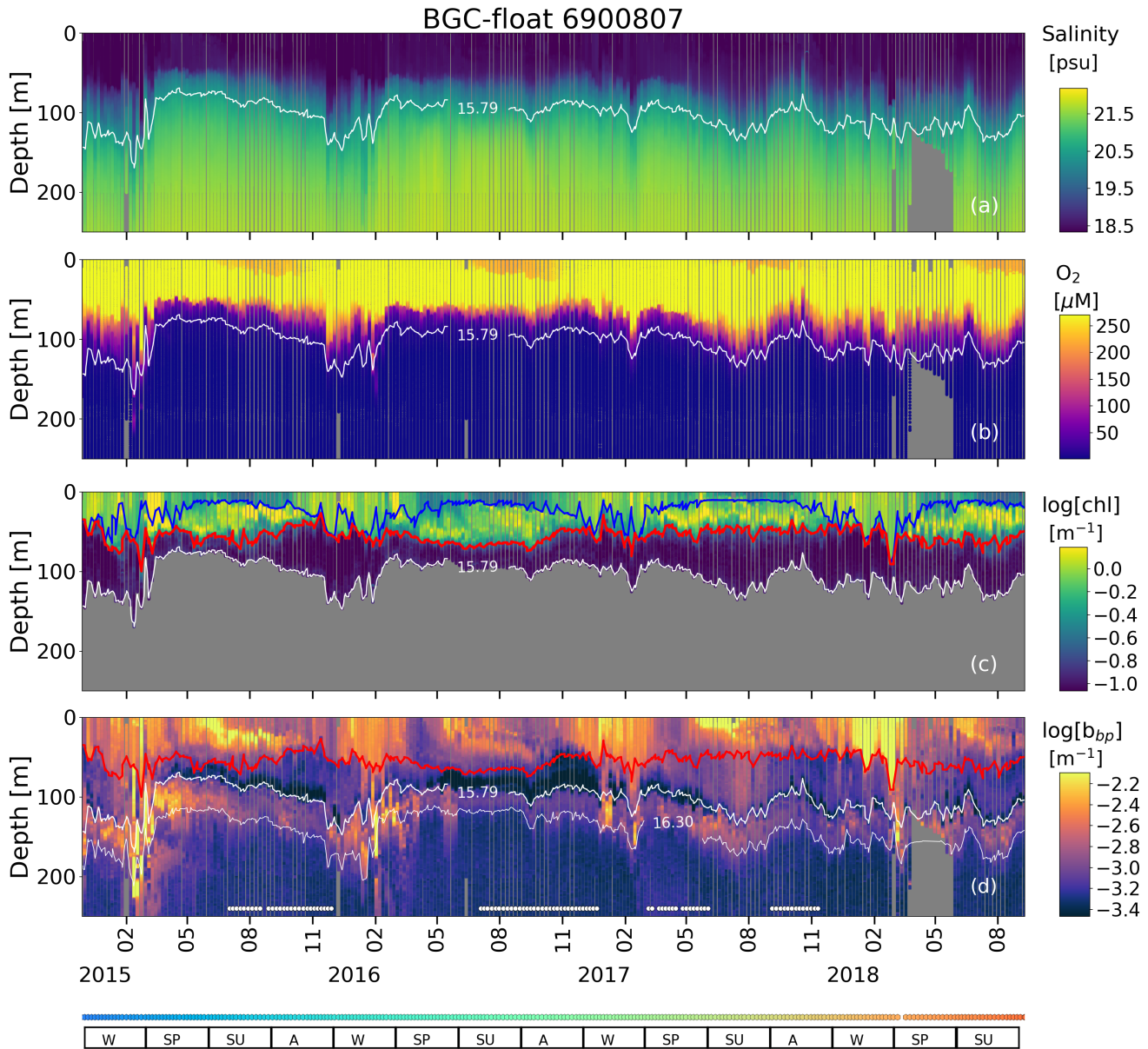
320 nitrate available to generate N_2 , respectively. Such variations in the characteristics of the b_{bp} -layer highlight that N_2 -production
321 rates can be highly variable in the Black Sea. We therefore propose that high resolution measurements of O_2 and b_{bp} can
322 potentially be exploited as a combined proxy to delineate the *effective* N_2 -yielding section of ODZs. This proposition is in part
323 supported by evidence that the b_{bp} -layer and a majority of N_2 -yielding microbial communities are both confined in the
324 shallower oxygen-poor water masses of ODZs. We however recommend investigation into the key biogeochemical drivers of
325 the b_{bp} -layer for each ODZ. This information will be critical for validating the applicability of the b_{bp} -layer in assessing spatial-
326 temporal changes in N_2 production.

327 Finally, it is evident that BGC-Argo float observations can acquire essential proxies of N_2 production and associated drivers
328 at appropriate spatial and temporal resolutions. The development of observation-modeling synergies therefore holds the
329 potential to deliver an unprecedented view of N_2 -yielding drivers if robotic observations become an integrated part of model
330 validation. Ultimately, this approach could prove essential for reducing present uncertainties in the oceanic N_2 budget.

331 Appendix A: Supplementary Figures



332
333 **Figure A1: Sampling locations of floats (a) 7900591 and (b) 6900807 between December 2013 and July 2019. Colored**
334 **squares and hexagons indicate the date (colorbar) for a given profile of floats 6900807 and 7900591, respectively.**



343
344 **Figure A3: Same as Figure A2 but for float 6900807**

345 *Data availability.* Data from Biogeochemical-Argo floats used in this study are freely available at <ftp.ifremer.fr/ifremer/argo>.
346 These data were collected and made freely available by the International Argo Program and the national programs that
347 contribute to it (<http://www.argo.ucsd.edu>; the Argo Program is part of the Global Ocean Observing System). Data on N₂:Ar
348 ratios are freely available at <https://agupubs.onlinelibrary.wiley.com/doi/abs/10.1029/2018GB006032>.

349 *Author contributions.* R.R. conceptualized the study, wrote the original draft, and generated all figures. H.C. contributed to
350 tuning the study's conceptualization and figures design. A.P. processed all BGC-Argo float data. R.R. and H.C. reviewed and
351 edited the final manuscript. **We finally thank Dr. Clara A. Fuchsman and the anonymous reviewer for their accurate and**
352 **constructive feedback, which allowed us to significantly improve the original version of the manuscript.**

353 *Acknowledgments.* This study was conducted in the framework of the *Noceanic* project. This project is funded by the European
354 Union's Horizon 2020 research and innovation program under the Marie Skłodowska-Curie Individual Fellowship awarded to

- 355 Rafael Rasse (grant agreement 839062). This study is a contribution to the remOcean project (European Research Council,
356 grant agreement 246777, Hervé Claustre).
- 357 *Competing interests.* The authors declare that they have no conflicts of interest.
- 358 **References**
- 359 Alldredge, A. L., and Cohen, Y.: Can microscale chemical patches persist in the sea? Microelectrode study of marine snow,
360 fecal pellets, *Science*, 235(4789), 689-691, DOI: 10.1126/science.235.4789.689, 1987
- 361 Altabet, M. A., Ryabenko, E., Stramma, L., Wallace, D. W., Frank, M., Grasse, P., and Lavik, G.: An eddy-stimulated hotspot
362 for fixed nitrogen-loss from the Peru oxygen minimum zone, *Biogeosciences*, 9, 4897-4908, [https://doi.org/10.5194/bg-9-](https://doi.org/10.5194/bg-9-4897-2012)
363 4897-2012, 2012
- 364 Babbin, A. R., Keil, R. G., Devol, A. H., and Ward, B. B.: Organic matter stoichiometry, flux, and oxygen control nitrogen
365 loss in the ocean, *Science*, 344(6182), 406-408, DOI: 10.1126/science.1248364, 2014.
- 366 Bianchi, D., Dunne, J. P., Sarmiento, J. L., and Galbraith, E. D.: Data-based estimates of suboxia, denitrification, and N₂O
367 production in the ocean and their sensitivities to dissolved O₂, *Global Biogeochem. Cy.*, 26(2), 2012.
- 368 Bianchi, D., Weber, T. S., Kiko, R., and Deutsch, C.: Global niche of marine anaerobic metabolisms expanded by particle
369 microenvironments, *Nat. Geosci.*, 11(4), 263-268, <https://doi.org/10.1038/s41561-018-0081-0>, 2018.
- 370 Bishop, J. K., and Wood, T. J.: Year-round observations of carbon biomass and flux variability in the Southern Ocean, *Global*
371 *Biogeochem. Cy.*, 23(2), <https://doi.org/10.1029/2008GB003206>, 2009.
- 372 Bittig, H. C., and Körtzinger, A. : Tackling oxygen optode drift: Near-surface and in-air oxygen optode measurements on a
373 float provide an accurate in situ reference, *J. Atmos. Ocean. Technol.*, 32(8), 1536-1543, [https://doi.org/10.1175/JTECH-D-](https://doi.org/10.1175/JTECH-D-14-00162.1)
374 14-00162.1, 2015.
- 375 Boyd, P. W., Claustre, H., Levy, M., Siegel, D. A., and Weber, T.: Multi-faceted particle pumps drive carbon sequestration in
376 the ocean, *Nature*, 568(7752), 327-335, <https://doi.org/10.1038/s41586-019-1098-2>, 2019.
- 377 Briggs, N., Perry, M. J., Cetinić, I., Lee, C., D'Asaro, E., Gray, A. M., and Rehm, E.: High-resolution observations of aggregate
378 flux during a sub-polar North Atlantic spring bloom, *Deep-Sea Res. Pt. I.*, 58(10), 1031-1039,
379 <https://doi.org/10.1016/j.dsr.2011.07.007>, 2011.
- 380 Briggs, N., Dall'Olmo, G., and Claustre, H.: Major role of particle fragmentation in regulating biological sequestration of CO₂
381 by the oceans, *Science*, 367(6479), 791-793, DOI: 10.1126/science.aay1790, 2020.
- 382 Bristow, L.A., Dalsgaard, T., Tiano, L., Mills, D.B., Bertagnolli, A.D., Wright, J.J., Hallam, S.J., Ulloa, O., Canfield, D.E.,
383 Revsbech, N.P. and Thamdrup, B. : Ammonium and nitrite oxidation at nanomolar oxygen concentrations in oxygen minimum
384 zone waters, *Proc. Natl. Acad. Sci. U. S. A.*, 113(38), 10601-10606, <https://doi.org/10.1073/pnas.1600359113>, 2016.
- 385 Bristow, L.A., Callbeck, C.M., Larsen, M., Altabet, M.A., Dekaezemacker, J., Forth, M., Gauns, M., Glud, R.N., Kuypers,
386 M.M., Lavik, G. and Milucka, J.: N₂ production rates limited by nitrite availability in the Bay of Bengal oxygen minimum
387 zone, *Nat. Geosci.*, 10(1), 24-29, <https://doi.org/10.1038/ngeo2847>, 2017.

388 Cavan, E. L., Trimmer, M., Shelley, F., & Sanders, R.: Remineralization of particulate organic carbon in an ocean oxygen
389 minimum zone, *Nat. Commun.*, 8(1), 1-9. <https://doi.org/10.1038/ncomms14847>, 2017.

390 Chang, B. X., Devol, A. H., and Emerson, S. R.: Denitrification and the nitrogen gas excess in the eastern tropical South
391 Pacific oxygen deficient zone, *Deep-Sea Res. Pt. I.*, 57(9), 1092-1101, <https://doi.org/10.1016/j.dsr.2010.05.009>, 2010.

392 Chang, B. X., Devol, A. H., and Emerson, S. R.: Fixed nitrogen loss from the eastern tropical North Pacific and Arabian Sea
393 oxygen deficient zones determined from measurements of N₂:Ar, *Global Biogeochem. Cy.*, 26(3),
394 <https://doi.org/10.1029/2011GB004207>, 2012.

395 Callbeck, C.M., Lavik, G., Ferdelman, T.G., Fuchs, B., Gruber-Vodicka, H.R., Hach, P.F., Littmann, S., Schoffelen, N.J.,
396 Kalvelage, T., Thomsen, S. and Schunck, H.: Oxygen minimum zone cryptic sulfur cycling sustained by offshore transport of
397 key sulfur oxidizing bacteria, *Nat. Commun.*, 9(1), 1-11, <https://doi.org/10.1038/s41467-018-04041-x>, 2018.

398 Canfield, D. E., and Thamdrup, B.: Towards a consistent classification scheme for geochemical environments, or, why we
399 wish the term 'suboxic' would go away, *Geobiology*, 7(4), 385-392. <https://doi.org/10.1111/j.1472-4669.2009.00214.x>, 2009.

400 Canfield, D.E., Stewart, F.J., Thamdrup, B., De Brabandere, L., Dalsgaard, T., Delong, E.F., Revsbech, N.P. and Ulloa, O.: A
401 cryptic sulfur cycle in oxygen-minimum-zone waters off the Chilean coast, *Science*, 330(6009), 1375-1378, DOI:
402 10.1126/science.1196889, 2010.

403 Clement, B. G., Luther, G. W., and Tebo, B. M.: Rapid, oxygen-dependent microbial Mn (II) oxidation kinetics at sub-
404 micromolar oxygen concentrations in the Black Sea suboxic zone, *Geochim. Cosmochim. Acta*, 73(7), 1878-1889.
405 <https://doi.org/10.1016/j.gca.2008.12.023>, 2009.

406 Codispoti, L. A.: An oceanic fixed nitrogen sink exceeding 400 Tg N a⁻¹ vs the concept of homeostasis in the fixed-nitrogen
407 inventory, *Biogeosciences*, 4, 233-253, <https://doi.org/10.5194/bg-4-233-2007>, 2007.

408 Codispoti, L. A., Brandes, J. A., Christensen, J. P., Devol, A. H., Naqvi, S. W. A., Paerl, H. W., and Yoshinari, T.: The oceanic
409 fixed nitrogen and nitrous oxide budgets: Moving targets as we enter the anthropocene?, *Sci. Mar.*, 65(S2), 85-105, 2007.

410 Çoban-Yıldız, Y., Altabet, M. A., Yılmaz, A., and Tuğrul, S.: Carbon and nitrogen isotopic ratios of suspended particulate
411 organic matter (SPOM) in the Black Sea water column, *Deep Sea Res. Part II Top. Stud. Oceanogr.*, 53(17-19), 1875-1892.
412 <https://doi.org/10.1016/j.dsr2.2006.03.021>, 2006.

413 Dall'Olmo, G., and Mork, K. A.: Carbon export by small particles in the Norwegian Sea, *Geophys. Res. Lett.*, 41, 2921-2927,
414 <https://doi.org/10.1002/2014GL059244>, 2014.

415 Dalsgaard, T., Stewart, F.J., Thamdrup, B., De Brabandere, L., Revsbech, N.P., Ulloa, O., Canfield, D.E. and DeLong, E.F.:
416 Oxygen at nanomolar levels reversibly suppresses process rates and gene expression in anammox and denitrification in the
417 oxygen minimum zone off northern Chile, *MBio.*, 5(6), e01966-14, 10.1128/mBio.01966-14, 2014.

418 Dalsgaard, T., Thamdrup, B., Farías, L., and Revsbech, N. P.: Anammox and denitrification in the oxygen minimum zone of
419 the eastern South Pacific, *Limnol. Oceanogr.*, 57(5), 1331-1346, <https://doi.org/10.4319/lo.2012.57.5.1331>, 2012.

420 de Boyer Montégut, C., Madec, G., Fischer, A. S., Lazar, A., and Iudicone, D.: Mixed layer depth over the global ocean: An
421 examination of profile data and a profile-based climatology, *J. Geophys. Res. Oceans*, 109(C12),
422 <https://doi.org/10.1029/2004JC002378>, 2004.

423 Dellwig, O., Leipe, T., Ma, C., Glockzin, M., Pollehne, F., Schnetger, B., Yakushev, E. V., and Bo, M. E.: A new particulate
424 Mn – Fe – P-shuttle at the redoxcline of anoxic basins, *Geochim. Cosmochim. Ac.*, 74, 7100–7115.
425 <https://doi.org/10.1016/j.gca.2010.09.017>, 2010.

426 DeVries, T., Deutsch, C., Primeau, F., Chang, B., and Devol, A.: Global rates of water-column denitrification derived from
427 nitrogen gas measurements, *Nat. Geosci.*, 5(8), 547-550, <https://doi.org/10.1038/ngeo1515>, 2012.

428 DeVries, T., Deutsch, C., Rafter, P. A., and Primeau, F.: Marine denitrification rates determined from a global 3-D inverse
429 model, *Biogeosciences*, 10(4), 2481-2496. <https://doi.org/10.5194/bg-10-2481-2013>, 2013

430 Ediger, D., Murray, J. W., and Yilmaz, A.: Phytoplankton biomass, primary production and chemoautotrophic production of
431 the Western Black Sea in April 2003. *J. Mar. Syst.*, 198, 103183, <https://doi.org/10.1016/j.jmarsys.2019.103183>, 2019.

432 Estapa, M. L., Feen, M. L., and Breves, E.: Direct observations of biological carbon export from profiling floats in the
433 subtropical North Atlantic, *Global Biogeochem. Cy.*, 33(3), 282-300, <https://doi.org/10.1029/2018GB006098>, 2019.

434 Fuchsman, C. A., Devol, A. H., Saunders, J. K., McKay, C., and Rocap, G.: Niche partitioning of the N cycling microbial
435 community of an offshore oxygen deficient zone, *Front. Microbiol.*, 8, 2384, <https://doi.org/10.3389/fmicb.2017.02384>, 2017.

436 Fuchsman, C. A., Kirkpatrick, J. B., Brazelton, W. J., Murray, J. W., and Staley, J. T.: Metabolic strategies of free-living and
437 aggregate-associated bacterial communities inferred from biologic and chemical profiles in the Black Sea suboxic zone. *FEMS*
438 *Microbiol. Ecol.*, 78, 586–603, <https://doi.org/10.1111/j.1574-6941.2011.01189.x>, 2011.

439 Fuchsman, C. A., Murray, J. W., and Konovalov, S. K.: Concentration and natural stable isotope profiles of nitrogen species
440 in the Black Sea, *Mar. Chem.*, 111(1-2), 90-105, <https://doi.org/10.1016/j.marchem.2008.04.009>, 2008.

441 Fuchsman, C. A., Murray, J. W., and Staley, J. T.: Stimulation of autotrophic denitrification by intrusions of the Bosporus
442 Plume into the anoxic Black Sea, *Front. Microbiol.*, 3, 257, <https://doi.org/10.3389/fmicb.2012.00257>, 2012b.

443 Fuchsman, C. A., Paul, B., Staley, J. T., Yakushev, E. V., and Murray, J. W.: Detection of transient denitrification during a
444 high organic matter event in the Black Sea, *Global Biogeochem. Cy.*, 33(2), 143-162, <https://doi.org/10.1029/2018GB006032>,
445 2019.

446 Fuchsman, C. A., Staley, J. T., Oakley, B. B., Kirkpatrick, J. B., and Murray, J. W.: Free-living and aggregate-associated
447 Planctomycetes in the Black Sea, *FEMS Microbiol. Ecol.*, 80(2), 402-416, <https://doi.org/10.1111/j.1574-6941.2012.01306.x>,
448 2012a.

449 Ganesh, S., Bristow, L. A., Larsen, M., Sarode, N., Thamdrup, B., and Stewart, F. J.: Size-fraction partitioning of community
450 gene transcription and nitrogen metabolism in a marine oxygen minimum zone, *ISME J.*, 9(12), 2682,
451 <https://doi.org/10.1038/ismej.2015.44>, 2015.

- 452 Ganesh, S., Parris, D. J., DeLong, E. F., and Stewart, F. J.: Metagenomic analysis of size-fractionated picoplankton in a marine
453 oxygen minimum zone, *ISME J.*, 8(1), 187, <https://doi.org/10.1038/ismej.2013.144>, 2014.
- 454 Gaye, B., Nagel, B., Dähnke, K., Rixen, T., and Emeis, K. C.: Evidence of parallel denitrification and nitrite oxidation in the
455 ODZ of the Arabian Sea from paired stable isotopes of nitrate and nitrite, *Global Biogeochem. Cy.*, 27(4), 1059-1071,
456 <https://doi.org/10.1002/2011GB004115>, 2013.
- 457 **Glaubitz, S., Labrenz, M., Jost, G., and Jürgens, K.: Diversity of active chemolithoautotrophic prokaryotes in the sulfidic zone**
458 **of a Black Sea pelagic redoxcline as determined by rRNA-based stable isotope probing, *FEMS Microbiol. Ecol.*, 74(1), 32-**
459 **41, <https://doi.org/10.1111/j.1574-6941.2010.00944.x>, 2010.**
- 460 **Grote, J., Jost, G., Labrenz, M., Herndl, G. J., and Jürgens, K: Epsilonproteobacteria represent the major portion of**
461 **chemoautotrophic bacteria in sulfidic waters of pelagic redoxclines of the Baltic and Black Seas, *Appl. Environ. Microbiol.*,**
462 **74(24), 7546-7551, DOI: 10.1128/AEM.01186-08, 2008.**
- 463 Gruber, N., and Sarmiento, J. L.: Global patterns of marine nitrogen fixation and denitrification, *Global Biogeochem. Cy.*,
464 11(2), 235-266, <https://doi.org/10.1029/97GB00077>, 1997.
- 465 Gruber, N., and Galloway, J. N.: An Earth-system perspective of the global nitrogen cycle, *Nature*, 451(7176), 293-296,
466 <https://doi.org/10.1038/nature06592>, 2008.
- 467 Hamme, R. C., and Emerson, S. R.: The solubility of neon, nitrogen and argon in distilled water and seawater, *Deep-Sea Res.*
468 *Pt. I.*, 51(11), 1517-1528, <https://doi.org/10.1016/j.dsr.2004.06.009>, 2004.
- 469 Helm, K. P., Bindoff, N. L., and Church, J. A.: Observed decreases in oxygen content of the global ocean, *Geophys. Res. Lett.*,
470 38(23), <https://doi.org/10.1029/2011GL049513>, 2011.
- 471 Jayakumar, A., Chang, B. X., Widner, B., Bernhardt, P., Mulholland, M. R., and Ward, B. B.: Biological nitrogen fixation in
472 the oxygen-minimum region of the eastern tropical North Pacific ocean, *ISME J.*, 11(10), 2356-2367,
473 <https://doi.org/10.1038/ismej.2017.97>, 2017.
- 474 Jensen, M. M., Kuypers, M. M., Gaute, L., and Thamdrup, B.: Rates and regulation of anaerobic ammonium oxidation and
475 denitrification in the Black Sea, *Limnol. Oceanogr.*, 53(1), 23-36, <https://doi.org/10.4319/lo.2008.53.1.0023>, 2008.
- 476 Johnson, K. S.: Manganese redox chemistry revisited. *Science*, 313(5795), 1896-1897, DOI: 10.1126/science.1133496, 2006.
- 477 **Johnson, K. S., Coale, K. H., Berelson, W. M., and Gordon, R. M.: On the formation of the manganese maximum in the oxygen**
478 **minimum, *Geochim. Cosmochim. Acta.*, 60(8), 1291-1299, [https://doi.org/10.1016/0016-7037\(96\)00005-1](https://doi.org/10.1016/0016-7037(96)00005-1), 1996.**
- 479
- 480 Johnson, K. S., Pasquero de Fommervault, O., Serra, R., D'Ortenzio, F., Schmechtig, C., Claustre, H., and Poteau, A.:
481 Processing Bio-Argo nitrate concentration at the DAC level, doi:10.13155/46121, 2018.
- 482 Karl, D. M., Church, M. J., Dore, J. E., Letelier, R. M., and Mahaffey, C.: Predictable and efficient carbon sequestration in the
483 North Pacific Ocean supported by symbiotic nitrogen fixation, *Proc. Natl. Acad. Sci. U. S. A.*, 109(6), 1842-1849,
484 <https://doi.org/10.1073/pnas.1120312109>, 2012.

- 485 Karl, D. M., Knauer, G. A., and Martin, J. H.: Downward flux of particulate organic matter in the ocean: a particle
486 decomposition paradox, *Nature*, 332(6163), 438-441, <https://doi.org/10.1038/332438a0>, 1988.
- 487 Karstensen, J., Stramma, L., and Visbeck, M.: Oxygen minimum zones in the eastern tropical Atlantic and Pacific oceans,
488 *Prog. Oceanogr.*, 77(4), 331-350, <https://doi.org/10.1016/j.pocean.2007.05.009>, 2008.
- 489 Keeling, R. F., and Garcia, H. E.: The change in oceanic O₂ inventory associated with recent global warming, *Proc. Natl. Acad.*
490 *Sci. U. S. A.*, 99(12), 7848-7853, <https://doi.org/10.1073/pnas.122154899>, 2002.
- 491 Kiko, R., Biastoch, A., Brandt, P., Cravatte, S., Hauss, H., Hummels, R., Kriest, I., Marin, F., McDonnell, A.M.P., Oschlies,
492 A. and Picheral, M.: Biological and physical influences on marine snowfall at the equator, *Nat. Geosci.*, 10(11), 852-858,
493 <https://doi.org/10.1038/ngeo3042>, 2017.
- 494 Kirkpatrick, J. B., Fuchsman, C. A., Yakushev, E., Staley, J. T., and Murray, J. W.: Concurrent activity of anammox and
495 denitrifying bacteria in the Black Sea, *Front. Microbiol.*, 3, 256, <https://doi.org/10.3389/fmicb.2012.00256>, 2012.
- 496 Kirkpatrick, J. B., Fuchsman, C. A., Yakushev, E. V., Egorov, A. V., Staley, J. T., and Murray, J. W.: Dark N₂ fixation: nifH
497 expression in the redoxcline of the Black Sea, *Aquat. Microb. Ecol.*, 82, 43-58. <https://doi.org/10.3354/ame01882>, 2018.
- 498 Konovalov, S.K., Luther, G.I.W., Friederich, G.E., Nuzzio, D.B., Tebo, B.M., Murray, J.W., Oguz, T., Glazer, B., Trouwborst,
499 R.E., Clement, B. and Murray, K.J.: Lateral injection of oxygen with the Bosphorus plume—fingers of oxidizing potential in
500 the Black Sea, *Limnol. Oceanogr.*, 48(6), 2369-2376, <https://doi.org/10.4319/lo.2003.48.6.2369>, 2003.
- 501 Konovalov, S. K., Murray, J. W., and Luther III, G. W.: Black Sea Biogeochemistry, *Oceanography*, 18(2), 24,
502 <https://doi.org/10.5670/oceanog.2005.39>, 2005.
- 503 Konovalov, S. K., Murray, J. W., Luther, G. W., and Tebo, B. M.: Processes controlling the redox budget for the oxic/anoxic
504 water column of the Black Sea, *Deep-Sea Res. Pt. II.*, 53(17-19), 1817-1841, <https://doi.org/10.1016/j.dsr2.2006.03.013>, 2006.
- 505 Kuypers, M.M., Sliemers, A.O., Lavik, G., Schmid, M., Jørgensen, B.B., Kuenen, J.G., Damsté, J.S.S., Strous, M. and Jetten,
506 M.S.: Anaerobic ammonium oxidation by anammox bacteria in the Black Sea, *Nature*, 422(6932), 608,
507 <https://doi.org/10.1038/nature01472>, 2003.
- 508 Lam, P., Jensen, M. M., Lavik, G., McGinnis, D. F., Müller, B., Schubert, C. J., Amann, R., Thamdrup, B., and Kuypers, M.
509 M.: Linking crenarchaeal and bacterial nitrification to anammox in the Black Sea, *Proc. Natl. Acad. Sci. U. S. A.*, 104(17),
510 7104-7109. <https://doi.org/10.1073/pnas.0611081104>, 2007.
- 511 Lam, P., Lavik, G., Jensen, M.M., van de Vossenberg, J., Schmid, M., Woebken, D., Gutiérrez, D., Amann, R., Jetten, M.S.
512 and Kuypers, M.M.: Revising the nitrogen cycle in the Peruvian oxygen minimum zone, *Proc. Natl. Acad. Sci. U. S. A.*,
513 106(12), 4752-4757, <https://doi.org/10.1073/pnas.0812444106>, 2009.
- 514 Lewis, B. L., and Luther III, G. W.: Processes controlling the distribution and cycling of manganese in the oxygen minimum
515 zone of the Arabian Sea, *Deep Sea Res. Part II Top. Stud. Oceanogr.*, 47(7-8), 1541-1561, [https://doi.org/10.1016/S0967-0645\(99\)00153-8](https://doi.org/10.1016/S0967-0645(99)00153-8), 2000.
- 517 Margolin, A. R., Gerringa, L. J., Hansell, D. A., and Rijkenberg, M. J.: Net removal of dissolved organic carbon in the anoxic
518 waters of the Black Sea, *Mar. Chem.*, 183, 13-24, <https://doi.org/10.1016/j.marchem.2016.05.003>, 2016.

519 Margolskee, A., Frenzel, H., Emerson, S., and Deutsch, C.: Ventilation pathways for the North Pacific oxygen deficient zone,
520 *Global Biogeochem. Cy.*, 33(7), 875-890. <https://doi.org/10.1029/2018GB006149>, 2019.

521 Martin, J. H., & Knauer, G. A.: VERTEX: manganese transport through oxygen minima; *Earth Planet. Sci.*, 67(1), 35-47m
522 [https://doi.org/10.1016/0012-821X\(84\)90036-0](https://doi.org/10.1016/0012-821X(84)90036-0), 1984

523 Murray, J. W., Codispoti, L. A., and Friederich, G. E.: Oxidation-reduction environments: The suboxic zone in the Black Sea,
524 In C. P. Huang, C. R. O'Melia, and J. J. Morgan (Eds.), *Aquatic chemistry: Interfacial and interspecies processes*, ACS
525 *Advances in Chemistry Series* (Vol. 224, pp. 157–176), Washington DC: American Chemical Society, 1995.

526 Murray, J. W., Fuchsman, C., Kirkpatrick, J., Paul, B., and Konovalov, S. K.: Species and $\delta^{15}\text{N}$ Signatures of nitrogen
527 Transformations in the Suboxic Zone of the Black Sea, *Oceanography.*, 18(2), 36-47, <https://doi.org/10.5670/oceanog.2005.40>,
528 2005.

529 Naqvi, S.W.A.: Geographical extent of denitrification in the Arabian Sea, *Oceanol. Acta*, 14(3), 281-290, 1991

530 Naqvi, S. W. A., Kumar, M. D., Narvekar, P. V., De Sousa, S. N., George, M. D., and D'silva, C.: An intermediate nepheloid
531 layer associated with high microbial metabolic rates and denitrification in the northwest Indian Ocean, *J. Geophys. Res.*
532 *Oceans*, 98(C9), 16469-16479, <https://doi.org/10.1029/93JC00973>, 1993.

533 Organelli, E., Dall'Olmo, G., Brewin, R. J., Tarran, G. A., Boss, E., and Bricaud, A.: The open-ocean missing backscattering
534 is in the structural complexity of particles, *Nat. Commun.*, 9(1), 1–11. <https://doi.org/10.1038/s41467-018-07814-6>, 2018.

535 Oschlies, A., Brandt, P., Stramma, L., and Schmidtko, S.: Drivers and mechanisms of ocean deoxygenation, *Nat. Geosci.*,
536 11(7), 467-473, <https://doi.org/10.1038/s41561-018-0152-2>, 2018.

537 Peters, B. D., Babbin, A. R., Lettmann, K. A., Mordy, C. W., Ulloa, O., Ward, B. B., and Casciotti, K. L.: Vertical modeling
538 of the nitrogen cycle in the eastern tropical South Pacific oxygen deficient zone using high-resolution concentration and isotope
539 measurements, *Global Biogeochem. Cy.*, 30(11), 1661-1681, <https://doi.org/10.1002/2016GB005415>, 2016.

540 Rasse, R., and Dall'Olmo, G.: Do oceanic hypoxic regions act as barriers for sinking particles? A case study in the eastern
541 tropical north Atlantic, *Global Biogeochem. Cy.*, <https://doi.org/10.1029/2019GB006305>, 2019.

542 Reed, A., McNeil, C., D'Asaro, E., Altabet, M., Bourbonnais, A., and Johnson, B.: A gas tension device for the mesopelagic
543 zone, *Deep Sea Res. Part I Oceanogr. Res. Pap.*, 139, 68-78. <https://doi.org/10.1016/j.dsr.2018.07.007>, 2018.

544 Schmechtig, C., Claustre, H., Poteau, A., and D'Ortenzio, F.: Bio-Argo quality control manual for the chlorophyll-a
545 concentration, (pp.1–13), *Argo Data Management*. <https://doi.org/10.13155/35385>, 2014.

546 Schmechtig, C., Poteau, A., Claustre, H., D'ortenzio, F., Giorgio Dall'Olmo, G., and Boss E.: Processing BGC-Argo particle
547 backscattering at the DAC level, <https://doi.org/10.13155/39459>, 2015.

548 Schmidtko, S., Stramma, L., and Visbeck, M.: Decline in global oceanic oxygen content during the past five decades. *Nature*,
549 542(7641), 335–339, <https://doi.org/10.1038/nature21399>, 2017.

550 Sorokin, Y. I.: *The Black Sea: ecology and oceanography*. 2002.

551 Spinrad, R. W., Glover, H., Ward, B. B., Codispoti, L. A., and Kullenberg, G.: Suspended particle and bacterial maxima in
552 Peruvian coastal waters during a cold water anomaly, *Deep-Sea Res. Pt. I.*, 36(5), 715-733, 1989.

553 Stanev, E. V., Grayek, S., Claustre, H., Schmechtig, C., and Poteau, A.: Water intrusions and particle signatures in the Black
554 Sea: a Biogeochemical-Argo float investigation, *Ocean Dyn.*, 67(9), 1119-1136, <https://doi.org/10.1007/s10236-017-1077-9>,
555 2017.

556 Stanev, E. V., Poulain, P. M., Grayek, S., Johnson, K. S., Claustre, H., and Murray, J. W.: Understanding the Dynamics of the
557 Oxic-Anoxic Interface in the Black Sea, *Geophys. Res. Lett.*, 45(2), 864-871, <https://doi.org/10.1002/2017GL076206>, 2018.

558 Stramma, L., Johnson, G. C., Sprintall, J., and Mohrholz, V.: Expanding oxygen-minimum zones in the tropical oceans.
559 *Science*, 320(5876), 655–658, <https://doi.org/10.1126/science.1153847>, 2008.

560 Stramski, D., Boss, E., Bogucki, D., and Voss, K. J.: The role of seawater constituents in light backscattering in the ocean.
561 *Prog. Oceanogr.*, 61(1), 27–56, <https://doi.org/10.1016/j.pocean.2004.07.001>, 2004.

562 Stramski, D., Reynolds, R. A., Kahru, M., and Mitchell, B. G.: Estimation of particulate organic carbon in the ocean from
563 satellite remote sensing, *Science*, 285(5425), 239-242, DOI: 10.1126/science.285.5425.239, 1999.

564 Stumm, W., and Morgan, J.J.: *Aquatic Chemistry: An Introduction Emphasizing Chemical Equilibria in Natural Waters*,
565 *Wiley-Interscience, New York, 1970.*

566 Thierry, V., Bittig, H., and Argo BGC Team.: Argo quality control manual for dissolved oxygen concentration. Version 2.0,
567 23 October 2018. 10.13155/46542, 2018.

568 Tsementzi, D., Wu, J., Deutsch, S., Nath, S., Rodriguez-R, L. M., Burns, A. S., Ranjan, P., Sarode, N., Malmstrom, R.R.,
569 Padilla, C.C., nad Stone, B. K.: SAR11 bacteria linked to ocean anoxia and nitrogen loss, *Nature.*, 536(7615), 179-183,
570 <https://doi.org/10.1038/nature19068>, 2016.

571 Tutasi, P., and Escribano, R.: Zooplankton diel vertical migration and downward C into the Oxygen Minimum Zone in the
572 highly productive upwelling region off Northern Chile, *Biogeosciences*, 17, 455–473, [https://doi.org/10.5194/bg-17-455-](https://doi.org/10.5194/bg-17-455-2020)
573 2020, 2020.

574 Ulloa, O., Canfield, D. E., DeLong, E. F., Letelier, R. M., and Stewart, F. J.: Microbial oceanography of anoxic oxygen
575 minimum zones, *Proc. Natl. Acad. Sci. U. S. A.*, 109(40), 15996-16003, <https://doi.org/10.1073/pnas.1205009109>, 2012.

576 Wang, W. L., Moore, J. K., Martiny, A. C., and Primeau, F. W.: Convergent estimates of marine nitrogen fixation, *Nature*,
577 566(7743), 205-211, <https://doi.org/10.1038/s41586-019-0911-2>, 2019.

578 Ward, B. B. How nitrogen is lost, *Science*, 341(6144), 352-353, DOI: 10.1126/science.1240314, 2013.

579 Ward, B.B., Devol, A.H., Rich, J.J., Chang, B.X., Bulow, S.E., Naik, H., Pratihary, A. and Jayakumar, A.: Denitrification as
580 the dominant nitrogen loss process in the Arabian Sea, *Nature*, 461(7260), 78-81, <https://doi.org/10.1038/nature08276>, 2009.

581 Ward, B. B., and Kilpatrick, K. A.: Nitrogen transformations in the oxic layer of permanent anoxic basins: the Black Sea and
582 the Cariaco Trench, In *Black Sea Oceanography*, Springer, Dordrecht, 111-124, https://doi.org/10.1007/978-94-011-2608-3_7,
583 1991.

584 Ward, B. B., Tuit, C. B., Jayakumar, A., Rich, J. J., Moffett, J., and Naqvi, S. W. A.: Organic carbon, and not copper, controls
585 denitrification in oxygen minimum zones of the ocean, *Deep-Sea Res. Pt. I.*, 55(12), 1672-1683,
586 <https://doi.org/10.1016/j.dsr.2008.07.005>, 2008.

587 Whitmire, A. L., Letelier, R. M., Villagrán, V., and Ulloa, O.: Autonomous observations of in vivo fluorescence and particle
588 backscattering in an oceanic oxygen minimum zone, *Opt. Express*, 17(24), 21, 992–22,004.
589 <https://doi.org/10.1364/OE.17.021992>, 2009.

590 Wojtasiewicz, B., Trull, T. W., Bhaskar, T. U., Gauns, M., Prakash, S., Ravichandran, M., and Hardman-Mountford, N. J.:
591 Autonomous profiling float observations reveal the dynamics of deep biomass distributions in the denitrifying oxygen
592 minimum zone of the Arabian Sea, *J. Mar. Syst.*, <https://doi.org/10.1016/j.jmarsys.2018.07.002>, 2018.

593 Yakushev, E. V., Pollehne, F., Jost, G., Kuznetsov, I., Schneider, B., and Umlauf, L.: Analysis of the water column oxic/anoxic
594 interface in the Black and Baltic seas with a numerical model, *Mar. Chem.*, 107(3), 388-410,
595 <https://doi.org/10.1016/j.marchem.2007.06.003>, 2007.

596 Yılmaz, A., Çoban-Yıldız, Y., Telli-Karakoç, F., and Bologa, A.: Surface and mid-water sources of organic carbon by
597 photoautotrophic and chemoautotrophic production in the Black Sea. *Deep Sea Research Part II: Topical Studies in*
598 *Oceanography*, 53(17-19), 1988-2004, *Deep Sea Res. Part II Top. Stud. Oceanogr.*, <https://doi.org/10.1016/j.dsr2.2006.03.015>,
599 2006.

Point by point response to the reviewers

First iteration-Major revision-[First reviewer]

Dear Dr. Clara A. Fuchsman

Thank you very much for providing your valuable time to review our manuscript. We also thank you for your constructive feedback because it allowed us to improve the original version of the manuscript. Please find below answers and related actions for all your comments and recommendations.

King regards,

Rafael Rasse
Hervé Claustre
Antoine Poteau

General Comment

In “The suspended small-particles layer in the suboxic Black Sea: a proxy for delineating the effective N₂-yielding section” by Rasse et al, the authors analyze particle back scattering, oxygen, HS- and nitrate float data from the Black Sea. The authors can thus delineate the suboxic zone of the Black Sea with the float, and see productivity and export events. The authors assume that the particle back scattering data in the suboxic zone indicates the presence of anammox and heterotrophic denitrifying bacteria. This assumption may be problematic in the Black Sea where it is known that there are high manganese oxide concentrations in the suboxic zone, and it is known that there is an organic matter maximum at the top of the sulfidic zone composed of S oxidizers. However, the data in this paper is useful. The writing just needs to be shifted.

Answer. We agree and understand the main reviewer’s concern about the interpretation of the *b_{bp}-layer*.

Actions taken. We changed the writing at the required sections, and added the information needed to explain the role that other particles (inorganic & biogenic) have on the formation of the *b_{bp}-layer*. We are confident you will find this revised version satisfactory (see details below).

Main Comment #1

Large issues.

The introduction needs a section at the beginning describing the Black Sea. This is particularly important because the Black Sea differs from oxygen deficient zones in several important ways. The Black Sea has a sulfidic zone. There are fluxes of reduced species out of the sulfidic zone: reduced S, ammonium, reduced manganese, and methane among other reduced species. Additionally, the zone above the sulfide is suboxic rather than anoxic. Oxygen deficient zones, on the other hand, are mid-water zones that have oxygenated water below them. They are truly anoxic (Revsbech et al., 2009). They don’t have fluxes of reduced species entering them. In fact, ammonium is usually below detection (Widner, Fuchsman, et al., 2018; Widner, Mordy, et al., 2018). In the Black Sea, the flux of ammonium from the sulfidic zone determines the importance of anammox and its place in the water column. A comparison of depth profiles of anammox bacteria, ammonium flux and N₂ gas can be seen in Fuchsman et al 2012a. Linkage between aerobic ammonium oxidation of the upward flux of ammonium and anammox can be found in (Lam et al., 2007) Additionally, the Black Sea is known to have an organic matter maximum in the redoxcline and quite a bit of information is known about this maximum. (see below) The authors have data from the Black Sea and they need to be more focused on understanding that unique system.

Answer. We agree, the Black Sea is an ecosystem that clearly differs from oxygen deficient zones as we indicated very briefly between lines 215-216 (original manuscript).

Action taken. We removed the phrase oxygen deficient zones (ODZs) from the introduction and sections required. Instead, we used the term: “poorly-oxygenated water masses” (e.g. O₂ < 3 uM), which refers to those water masses at which N₂ can be produced independently of the biogeochemical mechanisms driving it. Thus, including basins (e.g. Black Sea and Cariaco basin) and oxygen deficient zones (e.g. ETNP, ETSP, and AS).

We also included a “background section” to describe the key biogeochemical processes and associated inorganic-biogenic particles contributing to the formation of the *b_{bp}-layer* (see more details below).

654 The changes mentioned above are highlighted in yellow in the following lines of the new manuscript:
655 - term: “poorly-oxygenated water masses”: 1, 8, 23, 25, 30, 35, 40, 42, 49, 57, 60, 63, 64, 69...165, etc.
656 - background section: 71-99.

657 **Main Comment #2**

659 What can this float data tell us about the Black Sea? Are the particle maxima larger on the edges than in the middle
660 of the Sea? Is there a correlation between euphotic zone particles and size of the suboxic zone particle max? Are
661 particle flux events correlated to a season? Not that these particular questions need to be answered. At the moment,
662 this paper tells us things that we already know (there is a particle maximum between 3uM oxygen and 10 uM
663 sulfide), but I think it could easily tell us more.

665 **Answer.** We agree, there are many interesting aspects that can be easily explored with our data set.
666 However, such aspects are out of the scope of our study. In addition, we consider that our findings tell more than
667 a single maximum of particles between 3 uM O₂ and 10 uM sulphide. This is mainly because they highlight that
668 the *b_{bp}-layer* can be exploited as a combined proxy to efficiently *delineate and track* the effective N₂ yielding
669 section. The latter was in part demonstrated by the *novel and robust b_{bp} vs NO₃⁻* correlations computed with *high*
670 *spatial and temporal* resolutions. The data of optical particles maxima are only used as complementary information
671 to support our findings.

672 Finally, from our point of view, we consider that the key questions would be: how this optically derived
673 layer of suspended small-particles can be exploited – by first time- to improve current estimates of N₂ yielding via
674 the growing BGC-Argo float network? For instance, what does this *b_{bp}-layer* can tell us about how physical forcing
675 drive spatial-temporal changes in the location and thickness of the *effective N₂ yielding* sections of ODZs? What
676 can occur to the *b_{bp}-layer* and related N₂ yielding rates, if O₂ is injected from the bottom instead of Mn²⁺, NH₄⁺ or
677 H₂S? How can we exploit the latter two aspects to improve oceanic estimates of N₂ production? Overall, this work
678 is only a step forward to build the foundations that we need to achieve the main goal of our ongoing research. We
679 hope the reviewer can also understand our perspective.

680 **Action taken.** We did not take actions about this.

681 **Main Comment #3**

683 I think it is important to note that manganese oxides are quite abundant in the Black Sea and that manganese oxides
684 are also particles in the 0.2-20 um size range. Particle backscattering detects particles of all kinds. In the Black Sea,
685 both ammonium and Mn²⁺ have an upward flux from the sulfide zone. Anammox bacteria use the ammonium flux
686 to produce N₂ gas (Fuchsman et al 2012a) and the Mn²⁺ is oxidized to manganese oxides under very low oxygen
687 levels in the same zone (Clement et al., 2009). Thus excess N₂ gas and manganese oxides are correlated. That
688 correlation is not due to causation however. The authors need to consider how the manganese oxides affect their
689 results. See (Clement et al., 2009; Dellwig et al., 2010; Yakushev et al., 2009) for more information about
690 manganese oxides in the Black Sea.

692 **Answer.** We agree with the reviewer. The role of manganese oxides and its link with the suspended small
693 particles layer should be described better.

694 **Action taken.** The role of manganese oxides (mainly as MnO₂) was included in both the new “background
695 section” and discussion.

697 The changes indicated above are highlighted in yellow in the following lines of the new version:
698 - 71-99, 175-202, 209-235, 264-270.

700 **Main Comment #4**

703 **[a]** The ability to detect particles in the water is not a measurement that only exists on floats, but is also
704 present on CTD packages. Thus, let us look at a station in the Black Sea where we have all the relevant data
705 the Western Gyre station in 2005. **[b & c]** Here the maximum in organic C associated with microbes is found at
706 sigma theta 16.3 (Figure 1 Fuchsman et al 2011). The maximum in anammox bacteria at the same cruise/station is
707 at sigma theta 16.0-16.1 and the maximum in biologically produced N₂ gas is at sigma theta 15.9-16.3 (Fuchsman
708 et al 2012a Figure 1d). The maximum in MnO₂ is at sigma theta 15.85 (Fuchsman et al 2011 Figure 6c). There is
709 a small minimum in transmission from 15.8-15.85. The transmission signal corresponds to the manganese oxide
710 peak not the peak in anammox bacteria or organic matter. However, that particular station didn't have a large

711 organic matter signal in the redoxycline. From looking at the authors' data, I would guess that they often see the
712 organic matter maximum in the redoxycline. The organic matter maximum in the Black Sea redoxycline is from S
713 oxidizing bacteria, which may or may not be autotrophic denitrifiers (Glaubitx et al., 2010; Kirkpatrick et al., 2018).
714 These organic matter maxima can be dominated by S utilizing autotrophic denitrifiers of the genus Sulfurimonas
715 (Kirkpatrick et al., 2018 Figure 7). And thus they could be involved in N₂ production, but it has not been proven.
716 Some useful papers about the organic matter maximum in the redoxy- cline of the Black Sea (Coban-Yildiz et al.,
717 2006; Ediger et al., 2019; Glaubitx et al., 2010; Yilmaz et al., 2006).

718
719 **[d]** Though anammox and denitrification are very important biogeochemically, they aren't actually the
720 most abundant bacteria found in the Black Sea or oxygen deficient zones. In the ETNP oxygen deficient zone,
721 anammox bacteria reached 10% of the community and complete denitrifiers reach ~5% in the water and 14% of
722 the community on particles (Fuchsman et al., 2017). The most abundant bacteria in oxygen deficient zones, by far,
723 are nitrate reducing SAR11, reaching 60% of the community (Fuchsman et al., 2017; Tsementzi et al., 2016). In
724 the Black Sea, once again SAR11 are the most abundant bacteria (Fuchsman et al., 2011 Figure 2). The SAR11
725 cannot make N₂ gas. They just reduce nitrate to nitrite. I am just trying to note that for heterotrophic denitrifiers
726 and anammox, the authors are using a bulk measurement to look for changes in bacteria that are rarely more than
727 10% of the community.

728 **Answers.**

729 **[a] CTD.** We agree, CTD packages provide very valuable information about the physical, optical, and
730 biogeochemical properties of the ocean. For instance, they generate variables that cannot be measured by the
731 current float sensors as well as of those variables used to calibrate them. However, they can only provide a snapshot
732 for a given time of the sampling day, while discrete samples are often collected with poor vertical resolution. We
733 thus consider that alternative methods need to be developed to complement CTD packages, and ultimately better
734 understand biogeochemical cycles in poorly oxygenated regions as proposed here (please see also our answer in
735 the **main comment #1**, section 4.4. e.g. and refs: Chai et al., 2020; Claustre et al., 2020; Martin et al., 2020).
736
737

738 **Action taken.** We did not take actions about this.

739 **[b] Comparison between the vertical profiles of the particles measured by CTD and floats.** We
740 reviewed all figures and articles cited by the reviewer. Again, this is a very interesting description of the vertical
741 profiles of N₂, and particles using data collected via CTD packages. Even though we used the profile of March
742 2005 to highlight the *qualitative* relationship between N₂ excess and optical particles *only* in the *effective* N₂
743 production section; we consider these data are not the most suitable to compare the vertical profiles of particles
744 derived from CTD and floats (including those from Coban-Yildiz et al., 2006; Ediger et al., 2019; Glaubitx et al.,
745 2010; Yilmaz et al., 2006). The main reason is that the vertical profiles of particles cited by the reviewer are
746 representative of the region impacted by the Bosphorus plume. In this region, lateral advection via the Bosphorus
747 plume drives a maximum of particles ~ 16.3 kg m⁻³ (or higher) because it fuels chemoautotrophic activities by
748 injecting NO₃⁻ (e.g. ~ 700 m depth, Stanev et al. 2017). Thus, these CTD-profiles of particles must be similar to
749 those excluded in our analysis (e.g. see our Figure 2 between May-June). Note that we focus on the in-situ 1D
750 processes driving the local formation of the *b_{pp}-layer* (this was indicated between lines 83-84 of the original
751 manuscript). Thus, our data set is more representative of the profile described in Figures 1c-1d of Lam et al. 2017
752 indicated below. Also note that our *b_{pp}* maxima are located between the isopycnals 15.79 kg m⁻³ and 16.3 kg m⁻³
753 (Figure 2, and Figure 3g of the manuscript).
754

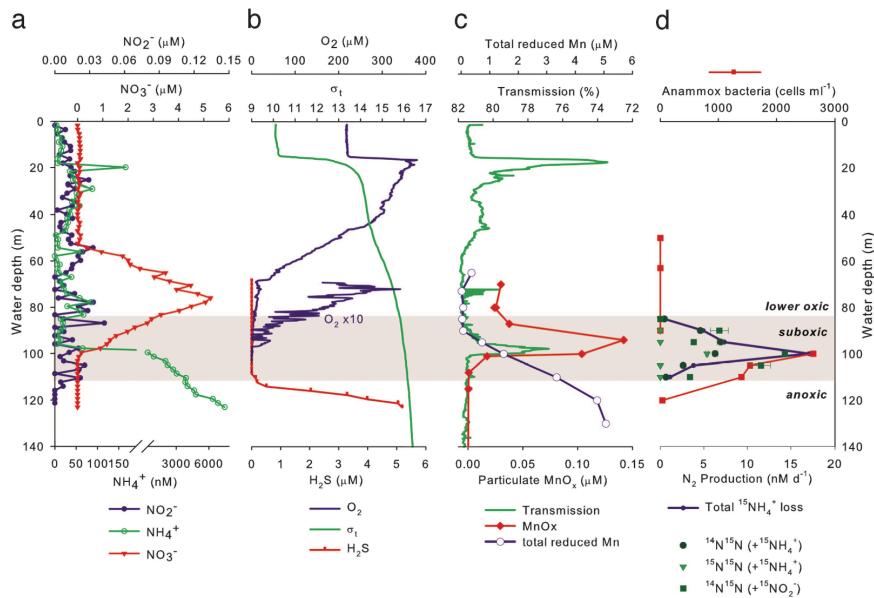
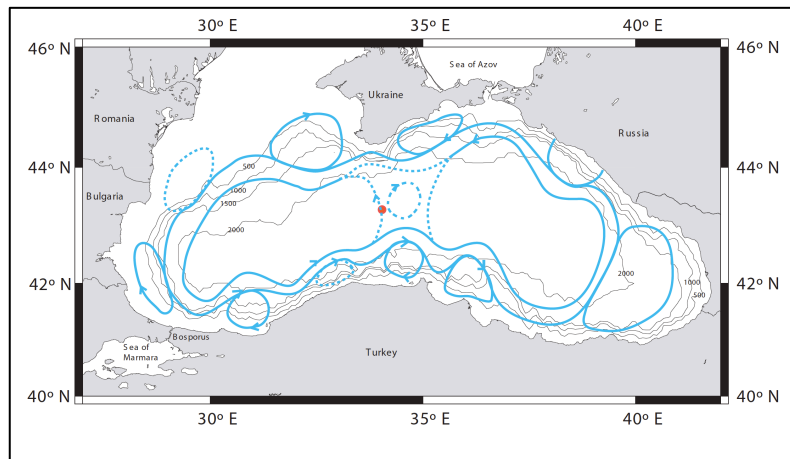


Fig. 1. Vertical distribution of inorganic nitrogen (a), O_2 and sulfide (b), light transmission, particulate MnO_x , and total reduced Mn (c), and anammox bacterial abundance and $^{15}\text{N}_2$ production rates (d).



Action taken. We did not take actions about this.

[c, d] Vertical profile of biogenic and organic particles. We thank the reviewer for this didactic and constructive comment.

Again, we agree. There are different biogenic and inorganic particles that contribute to the b_{bp} -layer, as we briefly recognize between lines 196-197 of the original manuscript. We only indicate that anammox-denitrifying bacteria are *at least partial contributors of the b_{bp} -layer* because they should have the major contribution to N_2 yielding and removal rates of NO_3^- . Hence, we did not suggest that such bacteria are the main microbial component (or organic particles) that contribute to the b_{bp} -layer. It is clear that b_{bp} signal is a black box that cannot be attributed to a single type of organic-inorganic particles.

As mentioned above, we are only trying to highlight two aspects: (1) the b_{bp} -layer is systematically *delineating* and *tracking* the effective N_2 yielding section, independently of the physical (e.g. NH_4^+ , Mn^{2+} , H_2S pumped from the sulfidic zone) and biogeochemical mechanisms driving both N_2 yielding and the small-particles content, and (2) similar results should also be expected for the b_{bp} -layer of the ODZ because this layer must be mainly due to the microbial communities involved in N_2 yielding (see also the answer of the **main comment # 1, section 4.4, and refs:** Martin and Knauer, 1984; Johnson et al., 1996; Lewis and Luther, 2000).

Action taken. We added information about the other inorganic and biogenic particles that contribute to the formation of the b_{bp} -layer, and modified the writing at the required sections.

Such changes are highlighted in yellow in the following lines of the new manuscript:

Main Comment #5

Thus, in the Black Sea, I think the assumption that the particle layer represents anammox and heterotrophic denitrifiers is not ideal. First, there are high concentrations of particulate metals in the Black Sea, particularly manganese oxides. Second, the organic matter maximum in the redoxcline is from S oxidizers. Some of these S-oxidizers may be autotrophic denitrifiers. Some aren't. Thus I think the way the particle maximum is talked about in the paper needs to be shifted. Additionally all this information should be in the introduction and discussion.

Answer. We agree

Action taken. We changed how the maximum of optical particles is described (see all details above and in the new version).

Specific [ES].

ES comment # 1

Was the oxygen data from the floats calibrated? See the work of Seth M. Bushinsky to understand the importance of calibration. This information is glossed over in the methods. I think that in previous float work in the Black Sea, scientists used the sulphide zone as a zero to at least track the drift of the oxygen optode over time. Also, it would be good to have a detection limit for all the different float sensors. Bushinsky et al 2016 Limnology and Oceanography Methods

Answer. Yes, the optodes 43330 are multi-point calibrated. The oxygen data is adjusted and corrected following the Argo quality control manual for dissolved oxygen concentration as cited in the manuscript (Thierry et al. 2018).

Action taken. We added both the range of O₂ concentrations that can be measured by the Optode sensors and their accuracy. This information is reported by the manufacturer. In addition, we cited the work related to the O₂ Optode Drift correction applied to the sensors (Bittig, and Körtzinger. 2015).

ES comment # 2

Line 8: This sentence is not accurate as written.

Answer. Agree

Action taken. We modified this sentence.

ES comment # 3

Line 22-23: I am confused what this sentence is trying to say. I note that N₂ gas concentrations can be between 400 and 500 microM in the water due to abiotic gas exchange of N₂ from the atmosphere. So the authors really mean to say N₂ production not concentration. The use of the word respectively in line 23 implies that denitrification is 20% of N₂ production and anammox is 40%. Rather, I think the authors are talking about how 20-40% of N₂ production occurs in the water column as opposed to in the sediments. The best citation for this is (DeVries et al., 2013).

Answer. We did not understand this observation because N₂ concentration is not mentioned in this sentence. We only indicate that N₂ is mainly produced via anammox-denitrification.

Action taken. We modified this sentence and removed the word "respectively".

ES comment # 4

Line 25: perhaps "where the bacteria that mediate the process mainly reside"

Answer. OK.

Action taken. We did not take actions about this because this is only a semantic issue.

ES comment # 5

Line 26-27: I am confused as to the meaning of this sentence? Are the authors trying to say that 90% of the N₂ production occurred in the upper ODZ? Perhaps it would be better to say that 90% of N₂ production occurred in the upper 50 meters of the ODZ. Additionally, one should either say N₂ production or N loss. N loss refers to the

836 loss of nutrients. The N₂ is produced not lost. I also note that anammox rates are not always highest at the top of
837 the ODZ. See (De Brabandere et al., 2014)

838 **Answer.** OK.

839 **Action taken.** The term ODZs was removed from the introduction. We now use the term “shallower poorly-
840 oxygenated water masses” and replaced the word “loss” by “yielding” throughout the manuscript.

841

842 **ES comment # 6**

843 Paragraph 1: I am having issues with oxygen deficient zones being called suboxic. The deficient part of oxygen
844 deficient zone implies that the system is anoxic. No oxygen. The word was coined to differentiate these anoxic
845 systems from suboxic systems which are called oxygen minimum zones.

846

847 **Answer.** We agree, the application of the term suboxic is not accurate and very confusing because the O₂ levels
848 used to define it can potentially overlap with hypoxic (O₂ < 60 uM, e.g. Stramma et al. 2008) and anoxic conditions
849 (O₂ < 1-2 uM). Example, for the Black Sea, the suboxic zone is set between O₂ levels ranging between 1.8 uM and
850 39 uM (Fuschman et al., 2011; Stanev et al., 2018 and references therein).

851

852 **Action taken.** We now use the term “poorly oxygenated water masses” to describe the section where N₂ is
853 effectively produced. We also introduced the term, “chemical zones” because this is more suitable (or accurate) to
854 explain the biogeochemical reactions that drive N₂ yielding and the small-particle content in the poorly oxygenated
855 water masses (Canfield and Thamdrup, 2009).

856

857 The changes indicated above are highlighted in yellow in the following lines of the new manuscript:

858

859 - Lines: 71-99, 209-235, and 209-235.

860

860 **ES comment # 7**

861 Line 93: The best citation is (Dalsgaard et al., 2014). The authors do cite this paper

862

863 later. To be consistent it should be noted here as well.

864

864 **Answer.** OK

865

865 **Action taken.** We cited Dalsgaard et al., 2014 as well.

866

866 **ES comment # 8**

867 Line 121-122: This sentence needs clarification for two reasons. The authors are comparing depth and density. The
868 Black Sea is much more consistent in density space than depth. It would be good to give the density range as well
869 as the depth in line 121. Additionally, the authors compare a depth where sulfide is 11 uM to a depth where it is 10
870 nM. It is not surprising that the 11 uM depth is deeper than the 10 nM depth. That’s an order of magnitude different
871 in concentration. What is the HS⁻ detection limit of the float?

872

873 **Answer.** OK

874

875 **Action taken.** We reported the detection limit of HS⁻, as well as the ranges of depth and density. We also modified
876 the sentence between lines 121-122 of the old manuscript.

877

877 **ES comment # 9**

878 Lines 133-148: The particle layer is between 3 uM oxygen and 11 uM sulfide. Both manganese oxides, and S
879 oxidizers are also found in this range as well as methane oxidizers (Kirkpatrick et al 2018 Figure 6D)– not just
880 anammox and denitrifiers. It is true however, that lots of microbial activity is occurring in this zone. These
881 processes also could all affected by intrusions of oxygen. Lines 142-144: This is interesting.

882

883 **Answer.** OK

884

885 **Action taken.** This sentence was modified. We included the presence of other bacteria and MnO₂, and described
886 their links with O₂ and NO₃⁻ levels according to the case.

887

887 Such changes are highlighted in yellow in the following lines of the new manuscript:

888

888 - Lines: 71-99, 175-202, 209-235, 264-270.

889

890

891

892

893
894 **ES comment # 10**
895 Line 150-151: This sentence is confusing. I am glad that the authors acknowledge manganese oxides existence.
896 However, manganese oxides are formed by manganese oxidizing bacteria not by denitrifiers. Perhaps autotrophic
897 denitrifiers and manganese oxides, as concepts, should be separated into two sentences
898

899 **Answer.** OK

900 **Action taken.** This sentence was removed.

901
902 **ES comment # 11**

903 Line 171: Are the authors that confident in their oxygen concentrations? This would only be true if the sensors are
904 calibrated. Can the optode see the difference between 0.2 uM and 0 uM??
905

906 **Answer.** Yes. According to the manufacturer
907 (https://www.aanderaa.com/media/pdfs/d378_aanderaa_oxygen_sensor_4330_4330f.pdf), the Optode sensors can
908 measure O₂ concentrations between 0 to 1000 uM with an accuracy of 1.5%. Thus, in theory, we should be able to
909 see the difference between 0.2 uM and 0 uM. However, the minimum value of O₂ measured by the sensor and used
910 in our calculation was 0.22 uM. Thus, we cannot confirm (or regret) that such sensors can see such difference.
911

912 **Action taken.** We added the range of O₂ concentrations and accuracy of the Optode sensor reported for the
913 manufacturer. Finally, we indicated that 0.22 uM was the minimum value of O₂ measured by the sensor, and
914 suggested that the O₂ level can be also lower (see line 224 in the new one)
915

916 **ES comment # 12**

917 Line 190: Can you actually differentiate correlations with temperature from correlations with density in these deep
918 layers? There is no biological reason that a change < 0.1 in temperature should matter. However, I think many
919 things, such as sulfide, correlate with temperature in this basin.
920

921 **Answer.** Correlations between b_{bp} vs T were computed between two reference isopycnals delineating the two sub-
922 zones of the b_{bp} -layer. The same principle was applied for b_{bp} vs NO₃⁻. Thus, these correlations are consistently
923 found in the water layers of the two sub-zones (or “chemical zones”) defined for the b_{bp} -layer. which ultimately
924 validates -in part- our main hypothesis. However, our data cannot explain why such correlation is found.
925

926 **Action taken.** The following sentence was added:

927
928 Finally, more information is needed to investigate the physical and/or biogeochemical processes driving the
929 correlation between the increase rates of T, and declines rates of NO₃⁻ in the first sub-zone. The former is, however,
930 out of the scope of our study. (lines 243-245 in the new version)
931

932 **ES comment # 13**

933 Line 235: (Cavan et al., 2018) Line 237: (Margolskee et al., 2019)

934 **Answer.** OK

935 **Action taken.** We cited Margolskee et al., 2019 and Cavan et al., 2017 because the latter is more suitable for this
936 context (see also Rasse and Dall’Olmo, 2019 for the ETNA-OMZ case; <http://dx.doi.org/10.1029/2019GB006305>).
937

938 **ES comment # 14**

939 3.4 New perspectives for studying N₂ losses in suboxic ODZs : This section would be
940 more compelling if the floats measured N₂ gas. There is such a device~A~TReed et al
941 2018 Deep Sea Research Part I 139: 68-78.
942

943 **Answer.** OK

944 **Action taken.** We cited Reed et al., 2018 and indicated that N₂ can be measured by BGC-floats.
945

946 **References not cited in the new version of the manuscript**
947

948 Chai, F., Johnson, K. S., Claustre, H., Xing, X., Wang, Y., Boss, E., ... & Sutton, A. (2020). Monitoring ocean
949 biogeochemistry with autonomous platforms. *Nature Reviews Earth & Environment*, 1-12.
950 <https://doi.org/10.1038/s43017-020-0053-y>

951
952 Claustre, H., Johnson, K. S., & Takeshita, Y. (2020). Observing the global ocean with biogeochemical-Argo.
953 *Annual Review of Marine Science*, 12, 23-48. <https://doi.org/10.1146/annurev-marine-010419-010956>

954
955 Stramma, L., Johnson, G. C., Sprintall, J., & Mohrholz, V. (2008). Expanding oxygen-minimum zones in the
956 tropical oceans. *science*, 320(5876), 655-658. DOI: 10.1126/science.1153847

957
958 Martin, A., Boyd, P., Buesseler, K., Cetinic, I., Claustre, H., Giering, S., ... & Robinson, C. (2020). The oceans'
959 twilight zone must be studied now, before it is too late. doi: 10.1038/d41586-020-00915-7

960
961 **Second iteration-Minor revision** -[First reviewer]

962 **General Comment**

963 I thank the authors for expanding the introduction and discussion to include manganese oxides as a source of
964 particles. I think this addition is important to the paper. However, the authors still need to add in references to
965 previous work on the organic matter maximum at the redox interface In the Black Sea. Just one or two sentences
966 acknowledging this previous work seems important since this organic matter maximum is the focus of the present
967 paper.

968 Important papers about the organic matter maximum in the Black Sea redoxyclyne: (Coban-Yildiz et al., 2006;
969 Yilmaz et al., 2006; Glaubitz et al., 2010; Ediger et al., 2019)
970 Perhaps add these new sentences around line 29 of the introduction.

971
972 First, we would like to thank Dr. Clara A. Fuschman for her constructive, positive, and accurate feedback. The
973 latter allowed us to improve the original version of this manuscript. We are confident that you will find this revised
974 version satisfactory.

975
976 **Answer.** We agree, Epsilonproteobacteria have the most significant contribution to the formation of organic
977 particles *mainly* in the sulfidic zone.

978
979 **Action taken.** We added the information related to the role of such bacteria in the formation of organic particles
980 and N₂ yielding. This information is in the section 2.0 between lines 83-88 of the last version (text highlighted in
981 green). Related references were also included.

982
983 **Specific [ES].**

984
985 **ES comment #1**

986 Line 31: N₂ yielding bacteria—the noun is necessary
987 Line 77: N₂ yielding bacteria

988
989 **Answer.** OK

990 **Action taken.** The noun N₂ yielding bacteria was added (text highlighted in green at lines 31 and 78, respectively)

991
992 **ES comment #2**

993 Poorly oxygenated isn't a scientific term. I think the term you are looking for is suboxic.

994
995 **Answer.** Oxygen-poor waters is a scientific term that was already used by Stramma et al. 2008 (abstract), 2010
996 (Introduction, 2nd paragraph). We thus consider that the latter term is equivalent to the one used here (poorly-
997 oxygenated).

998
999 **Action taken.** To be consistent with what is reported in the literature, we changed the terms poorly-oxygenated by
000 oxygen-poor throughout the manuscript. These changes are highlighted in green at the respective lines of the
001 revised manuscript.

002
003 **ES comment #3**

004 **Line 174:** The epsilonproteobacteria Sulfurimonas is one of the most important sulfur oxidizers in the Black Sea.
005 See (Glaubitz et al., 2010) also (Kirkpatrick et al., 2018) figure 7. This epsilon proteobacteria is likely an
006 autotrophic denitrifier (Fuchsman et al., 2012). Might be a better sulfur oxidizer to single out than SUP05—or
007 name them both.

008
009 **Answer. OK**

010 **Action taken.** We included the information requested between lines 178-179 of the revised manuscript (highlighted
011 in green).

012
013 **ES comment #4**

014 Line 28: the fact that some SAR11 can reduce nitrate is from (Tsementzi et al., 2016). I know you cite this paper
015 later, but it would be good to cite it here too.

016
017 **Answer. OK**

018 **Action taken.** The reference was included at the line specified.

019
020 **ES comment #5**

021 Line 312: Actually, your results do not suggest that the particle layer is due to the list of bacteria. Previous work
022 suggests this. For example (Glaubitz et al., 2010) or (Kirkpatrick et al., 2018). You assume that this is the case.
023 Please rephrase.

024
025 **Answer. OK**

026 **Action taken.** This sentence was rephrased.

027
028 **References**

029 Stramma, L., Johnson, G. C., Sprintall, J., & Mohrholz, V. (2008). Expanding oxygen-minimum zones in the
030 tropical oceans. *science*, 320(5876), 655-658. DOI: 10.1126/science.1153847

031
032 Stramma, L., Schmidtko, S., Levin, L. A., & Johnson, G. C. (2010). Ocean oxygen minima expansions and their
033 biological impacts. *Deep Sea Research Part I: Oceanographic Research Papers*, 57(4), 587-595.
034 <https://doi.org/10.1016/j.dsr.2010.01.005>

035
036

037 **First iteration-Minor revision**-[Second reviewer]

038 Dear reviewer,

039
040 Thank you very much for spending part of your valuable time reviewing our manuscript. We also thank you for
041 your constructive feedback because it allowed us to improve the original version of the manuscript. Below, you
042 will find our answers and actions taken for each of your comments.

043
044 King regards,

045
046 Rafael Rasse
047 Hervé Claustre
048 Antoine Poteau

049
050 **Specific [ES].**

051
052 **ES comment #1**

053
054 What is the typical depths ??

055
056 Are these depths vary among different ODZs?

057
058 **Answer. OK**

059
060 **Action taken.** This sentence was modified. We indicated the depths at which this layer can be found. This
061 information is based on data from the Black Sea (this study), and the ODZs of the Arabian Sea and ETSP (Whitmire
062 et al. 2009; Wojtasiewicz et al. 2018).

063
064 **ES comment #2**

065
066 Are these factors listed in order of their importance?

067
068 **Answer.** According to the literature, we consider this is the most likely order.

069
070 **Action taken.** We did not take actions about this.

071
072 **ES comment #3**

073
074 Will not the chemical composition, salinity and temperature of water column would also matter for resultant optical
075 visibility / abundance of anammox and denitrifying bacteria ??

076
077 **Answer.** Organic matter composition should be key driving the microbial activity (e.g. anammox and denitrifying
078 bacteria, e.g. Van Mooy et al. 2002) but this not be critical for our case (see line 165 in the old manuscript and the
079 cited work). We mentioned an array of chemical variables (levels O₂, NO₃, and HS, OM) at the line 34 of the old
080 version. We don't have information about salinity but T can affect their activity in sediments (e.g. Rysgaard et al.
081 2004; Canion et al., 2014).

082
083 **Action taken.** We did not take actions about this.

084
085 **ES comment #4**

086
087 Here authors are attempting to investigate measured Bbp layer (absorption ?) with chemical parameters such as
088 O₂, NO₃ H₂S and N₂ produced.....all chemical parameters is there any way to provide Bbp thickness and its
089 absorption correlation with actual density of microbial mass...(just wondering samples collected on filters??)

090
091 **Answer.** We did not have such data .

092 **Action taken.** We did not take actions about this.

093
094 **ES comment #5**

095
096 How much thick it is?

097
098 **Answer.** It can be highly variable with time, and between ODZs and anoxic basins. Please see section 4.1, where
099 we indicate the thickness of the *b_{bp}-layer* for the case of the Black Sea.

100
101 **Action taken.** We did not take actions about this..

102
103 **ES comment #6**

104
105 Suppose this factor is negligible in some locations ??

106
107 **Answer.** Please, see how the ventilation of subsurface O₂ defines the characteristics of the *b_{bp}-layer* and how we
108 used such information to explain what are the main particles contributing to its formation (e.g. section 4.2).

109
110 **Action taken.** We did not take actions about this.

111
112 **ES comment #7**

113
114 why ? what is another factor for second sub-zone?

115
116 **Answer.** This is related to the biogeochemical processes that control the content of suspended small particles and
117 N₂ excess in the chemical zones of the poorly-oxygenated water masses. This is better described in the new version
118 of the manuscript.

119
120 **Action taken.** We included a new “background section” to describe the key biogeochemical processes and
121 associated inorganic-biogenic particles contributing to the formation of the *b_{bp}-layer*. The interlinks among
122 biogeochemical processes, and the vertical profiles of small-particles and N₂ excess are described in the discussion
123 as well.

124
125 These changes are highlighted in yellow in the following lines of the new version:
126 - 71-99, 175-202, 209-235, 264-270..

127
128 **ES comment #8: Sentences highlighted in yellow without suggestions**

129
130 - of chl and bbp and due to particle

131
132 **Answer.** Both spikes are due to particles-aggregates. We thus consider this sentence is OK

133
134 **Action taken.** We did not take actions about this.

136
137
138 - hypothesized

139
140 - Optical proxies of tiny particles can be applied as an alternative approach to assess the vertical distribution of N₂-
141 yielding microbial communities in upper suboxic ODZs

142
143 - particle content inferred from bbp and N₂ produced by microbial communities are at least qualitatively correlated
144 microbial communities in upper suboxic ODZs

145
146 - bbp and O₂ can be exploited as a combined proxy for defining the N₂-producing section of the suboxic Black
147 Sea

148
149 - fluorescence and total backscattering were converted into Chlorophyll concentration (*chl*) and particle
150 backscattering (*b_{bp}*) following standard protocols

151
152 - HS- was not used to delimit the bottom of this zone because the maximum concentration of H₂S that denitrifying
153 and anammox bacteria tolerate is not well established.

154
155 - NO₃⁻ and O₂ are two of the key factors that modulate the presence of denitrifying and anammox bacteria

156
157 - bbp-layer is partially composed of N₂-yielding microbial communities such as anammox and denitrifying
158 bacteria.

159
160 - bbp-layer is at least partially composed of anaerobic microbial communities involved in the production of N₂

161
162 **Answer.** OK

163
164 **Action taken.** The sentences above were modified.

166
167 - o free-living bacteria (0.2-2 μm), and those associated with small-suspended particles (> 2-20 μm).

168
169 **Answer.** This particle size is explained in the introduction

170

171 **Action taken.** We did not take actions about this.

172

173 **ES comment #9: Other sentences highlighted in yellow without suggestions**

174

175 - How key drivers of anammox-denitrifying bacteria dynamics impact on the vertical distribution of bbp and the
176 thickness of the bbp-layer.

177

178 - Optical proxies of tiny particles can be applied as an alternative approach to assess the vertical distribution of N₂-
179 yielding

180

181 - Slightly sulfidic conditions of the deepest isopycnal at which anammox bacteria can be still recorded

182

183 - It is still debated whether the oceanic nitrogen cycle is in balance or not

184

185 **Answers.** Because it is not specified what are the issues with the sentences above; we assumed that these are only
186 semantic issues.

187 **Action taken.** We did not take actions about this.

188

189 **References.**

190 Canion, A., Kostka, J. E., Gihring, T. M., Huettel, M., Van Beusekom, J. E. E., Gao, H., ... & Kuypers, M. M.
191 (2014). Temperature response of denitrification and anammox reveals the adaptation of microbial communities to
192 in situ temperatures in permeable marine sediments that span 50° in latitude. *Biogeosciences*, 11(2), 309.

193

194 Rysgaard, S., Glud, R. N., Risgaard-Petersen, N., & Dalsgaard, T. (2004). Denitrification and anammox activity in
195 Arctic marine sediments. *Limnology and Oceanography*, 49(5), 1493-1502.

196

197 Whitmire, A. L., Letelier, R. M., Villagrán, V., and Ulloa, O.: Autonomous observations of in vivo fluorescence
198 and particle backscattering in an oceanic oxygen minimum zone, *Opt. Express*, 17(24), 21, 992–22,004.
199 <https://doi.org/10.1364/OE.17.021992>, 2009.

200 Wojtasiewicz, B., Trull, T. W., Bhaskar, T. U., Gauns, M., Prakash, S., Ravichandran, M., and Hardman-
201 Mountford, N. J.: Autonomous profiling float observations reveal the dynamics of deep biomass distributions in
202 the denitrifying oxygen minimum zone of the Arabian Sea, *J. Mar. Syst.*,
203 <https://doi.org/10.1016/j.jmarsys.2018.07.002>, 2020.

204 Van Mooy, B. A., Keil, R. G., & Devol, A. H. (2002). Impact of suboxia on sinking particulate organic carbon:
205 Enhanced carbon flux and preferential degradation of amino acids via denitrification. *Geochimica et*
206 *Cosmochimica Acta*, 66(3), 457-465.